WATER RESOURCES research center

Publication No. 81

ANALYSIS OF INJECTION IN STRATIFIED AQUIFERS

By

Steven J. Laux

And

Barry A. Benedict

Department of Civil Engineering
University of Florida
Gainesville

1984

UNIVERSITY OF FLORIDA

ANALYSIS OF INJECTION IN STRATIFIED AQUIFERS

By

Steven J. Laux

and

Barry A. Benedict

Publication No. 81

Florida Water Resources Research Center

Research Project Technical Completion Report

Project Number 371002

Annual Allotment Agreement Number

G-835

Report Submitted: August 1984

The research on which this report is based was financed in part by the U. S. Department of the Interior, as authorized by the Water Research and Development Act of 1978 (P.L. 95-457).

ACKNOWLEDGEMENTS

This project was sponsored by the Florida Water Resources Research Center with funds provided by the United States Department of the Interior and the United States Geological Survey as project no. 381002.

The computer facilities of the Northeast Regional Data Center of the State University System of Florida were used for this work.

The authors acknowledge the significant contribution to this work by Donnie Ellington whose efforts included computer work, drafting and proofreading. Thanks go to Lisa Rossignol and Debbie Butler for typing.

TABLE OF CONTENTS

LIST OF TABLES

LIST OF FIGURES

LIST OF SYMBOLS

BO	thickness of the semi-confining layer
B1	thickness of the aquifer
C	salt concentration
C_o	characteristic concentration
D	dispersion coefficient
F(n)	distribution function for specific discharge
h	depth below or above sea level
K	permeability of the aquifer
K_{sc}	permeability of the semi-confining layer
L(n)	distribution function for concentration
m	time level
n	porosity of the aquifer
P	pressure
q	specific discharge
r	radius of a point from a well
s	drawdown or head build up
S	storativity of the aquifer
T	transmissivity of an aquifer
t	time
U	characteristic specific discharge in the x-direction
u	component of specific discharge in the x-direction
V	characteristic specific discharge in the y-direction
v	component of specific discharge in the y-direction
w	vertical component of specific discharge
Z	vertical coordinate

α	constant relating salt concentration with unit weight
β	defined in Equation (4.34)
γ	unit weight of water
γ_o	unit weight of reference
δ	thickness of the transition zone
η	dimensionless coordinate within the transition zone
κ	solute convection
λ	leakage coefficient
ξ	buoyancy term defined in Equation (4.18b)
ρ	density
σ	storage term
ϕ	piezometric head
ψ	dispersion term

Subscripts

b	bottom of transition zone
f	freshwater
i	x-direction coordinate
j	y-direction coordinate
o	initial or reference condition
s	salt
t	top of transition zone

Superscripts

$\rightarrow$	vector
$\sim$	tensor
m	time level

ABSTRACT

An extension of the integral method was made to model the case of injection into a two-layer system with injection into the top of the lower layer. An alternating direction implicit (ADI) finite-difference model was developed to solve the equations describing this system. The need for small time steps for model convergence and the rapid stabilization of drawdowns led to the alternative use of an analytical method (the Hantush equation for leaky aquifers) to calculate drawdowns and drastically reduce computer time.

Attempts were made to fit the model to data from injection wells in Pinellas County, Florida. The basic extent of the injected water field was reproduced fairly well, except that the drawdown and injected water thickness in the immediate vicinity of the well are too small. Neglect of vertical flows in the well region may be of importance here. The complicated system here, with salt water both above and below the injected water, makes it difficult to estimate well concentrations currently.

The model developed in this work produces a tool for analysis of injections of wastes which should prove useful for preliminary assessments. Work is continuing to further the development and test against other data.

CHAPTER 1

INTRODUCTION

1.1 Description of Problem

Many coastal areas have density-stratified, artesian groundwater fields due to underlying saltwater and overlying freshwater, all held in a series of aquifers and semi-confining beds. In recent years, these saline aquifers have been used in deep injection disposal of treated sewage and industrial waste. Potential benefits or hazards to groundwater resources could result from this practice.

Treated freshwater sewage could possibly be injected into coastal areas in an effort to stop the landward movement of saltwater intrusion. This also provides a convenient method of disposing of treated sewage. Also, surface runoff and excess potable surface water could be injected into a saline aquifer during rainy seasons and periods of excess surface water. Later, during dry periods with little rainfall, the previously injected water would be pumped from the aquifer for potable use. This practice may prove beneficial in many coastal areas of Florida where saltwater intrusion has currently eliminated groundwater as a potable water resource.

There are also potential hazards associated with deep-well injection. This is a management technique where the technology is still very young and the long-term effects of injecting pollutants into an aquifer are still not well known.

Experts in this field still feel that they are working in an unknown area when they pump pollutants into an aquifer. In aquifers of low permeability, where water velocities are very low, undesirable changes to an aquifer due to injection may go undetected until the damage is already extensive. Also, in very low permeabily aquifers, any changes may be essentially "irreversible", making it impossible to undo any undesirable effects of pollutant injection.

Today, in Florida, there are over fifty injection wells that are owned and operated by municipal water treatment plants, power plants, industrial plants, and agricultural cooperatives. The majority of injection wells in Florida are used for disposal of sanitary sewage. With these wells in existence and with the increasing popularity of injection disposal of waste, the risk of extensive damage to potable water aquifers increases. If migration of pollutants is not anticipated correctly, the pollutants could appear in areas where it is undesirable.

It has long been recognized that a tool is needed to predict the effects of injecting a lighter fluid into a heavier fluid. It is the objective of this work to discuss several modeling methods available and to develop one or more of these techniques for use by persons involved in deep-well injection.

The goal is to develop a numerical, or semi-numerical, scheme for the prediction of effects of an injection well, or a series of injection wells, on an aquifer. It is desired to create such a program that would be usable by consulting firms and regulatory agencies; to this end, it is desired that the computer capacity requirements are small enough that modeling could take place on a micro-computer. This would put advanced modeling techniques within the grasp of persons previously not able to afford them.

1.2 Methodology

To develop a usable model of an injection well in a salt-water aquifer it will first be necessary to review the existing groundwater modeling literature. There is much information about the saltwater intrusion problem, which has some similarity to the injection situation. Unfortunately, even most current stratified groundwater-flow models make the simplifying assumption of a sharp interface between the freshwater and saltwater. The actual change from fresh to saltwater occurs through a transition zone of varying density and salt concentration. It is desirable to locate the transition zone and use it to calculate salt concentrations within the pumping region.

Benedict, Rubin, and Means [1983] developed a three-dimensional saltwater upconing model that accounted for the transition zone using an integral technique. This model could be modified and the theory extended to simulate the injection problem. Although this model uses much less computer time than large-scale numerical models, several simplifying assumptions, based on analysis of the basic equations, could be made to further reduce its run-time cost. It has been observed that in the upconing model there are some numerical problems encountered in the transition zone calculations. These and other problems must be worked out before a modification of the upconing model could be considered.

Once a model has been developed, it will be necessary to compare its output to actual injection well field-data. Suitable data has been obtained from a U.S. Geological Survey report on several injection wells in the Pinellas County, Florida area.

Once the validity of the model has been verified, the model will tested to establish limits for numerical convergence and stability, well as model sensitivity to input parameters, as well as defini limits of model applicability. The final model should provide a usef tool for assessment of injection well impact, while at the same ti being of a scale and cost as to be useful to many professionals.

CHAPTER 2

LITERATURE REVIEW

2.1 Introduction

In this chapter a review will be made of available literature covering stratified groundwater flow as it applies to the injection situation. Injection of freshwater into a saltwater aquifer is a phenomenon that is somewhat analogous to that of saline intrusion due to pumping. For this reason, and because there is less specific information available about injection modeling, part of the literature review will be of the saltwater intrusion situation.

2.2 Magnitude of Problem

Injection wells have been of interest in this country for years. They have been conceived as a means of waste disposal; as a means of recharging aquifers; as a means of increasing local piezometric heads, thereby reducing potential for salt water intrusion; or as some combination of these. Of particular concern is Florida, where the large coastal region offers many possibilities for injection into saline regions. Helpling [1980] noted that in 1980 at least ninety-one injection wells were being considered, planned, or were in operation in Florida. CH_2M Hill [1983] lists a large number of such sites, probably representing about 75 percent of existing injection sites in Florida. Table 2.1 lists wells in Florida to give an indication of the types of injection wells existing.

2.3 Analytical Studies

An analytical technique for calculating the shape of a sharp, fresh-saline water interface was developed by Ghyben [Ghyben 1888] and

Location	Number of Wells, (Diameter) Injection	Monitor	Well Depth (ft)	Year Completed	Remarks
Sugar Cane Growers Cooperative of Florida	2 (8")	1 (6")	2,000	1966	Operated 1966-76 Superseded by wells for The Quaker Oats Co. (See listing below) Industrial effluent
General Waterworks Corporation	2 (16")	-	3,100	1970	Sunset Park & Kendale Lakes Operating since 1971 in Dade Co.
				1971	Secondary treated sanitary effluent Replaced by Miami-Dade Water and Sewer Authority system February 1983 (See listing below)
American Cyanamid	1 (6")	-	1,547	1971	Santa Rosa Plant Test will for industrial effluent
The Quaker Oats Company	3 (10")	3 (6")	3,300	1977	Operating since 1978 Industrial effluent
City of Margate	1 (24")	1 (9-5/8")	3,200	1974	Operating since 1974 Secondary treated sanitary effluent
Florida Power & Light Co.	1 (12")	-	1,500	1974	Willow Plant Exploratory well Underground storage
Florida Power & Light Co.	1 (12")	-	1,600	1974	Palatka Plant Exploratory well Industrial effluent
City of Sarasota	1 (16")	-	3,000	1974	Exploratory well Secondary treated sanitary effluent
City of Stuart	1 (16") 1 (10")	1 (8")	3,000 3,300	1975 1982	Secondary treated sanitary effluent

Table 2.1 SOME INJECTION WELLS IN THE STATE OF FLORIDA

Location	Number of Wells, (Diameter) Injection	Monitor	Well Depth (ft)	Year Completed	Remarks
City of Stuart, Continued					Installed additional 10-inch casing by order of FDER and deepened to 3,300 feet in 1982
City of Gainesville	4 (30")	10 (4")	1,000	1976	Operating since 1976 Advanced treated sanitary effluent
City of St. Petersburg	3 (16")	5 (8")	1,000	1977	S.W. Plant Operating since 1977 Secondary treated sanitary effluent with filtration
City of St. Petersburg	3 (20")	5 (8")	1,000	1978	N.E. Plant Operating since 1980 Secondary treated sanitary effluent with filtration
City of St. Petersburg	2 (20")	1 (6")	-	-	N.W. Plant Design completed-construction scheduled for 1983 Secondary treated sanitary effluent with filtration
Hercules, Inc.	1 (10")	1 (6")	3,005	1979	Operating since 1979 Industrial effluent
Miami-Dade Water and Sewer Authority (MDWSA)	8 (24") 1 (20")	3 (6")	3,100 3,100	1981 1981	South District Plant Secondary treated sanitary effluent
General Development Utilities	1 (12")	1 (6")	3,400	1983	Port St. Lucie Secondary treated sanitary effluent
City of Sunrise	2 (24")	1 (6")	3,200	1984	Secondary treated sanitary effluent

Table 2.1 SOME INJECTION WELLS IN THE STATE OF FLORIDA Continued

Herzberg [Herzberg 1901]. The Ghyben-Herzberg relationship assumes horizontal streamlines in the freshwater and no movement in the saltwater. It has been widely applied to problems where vertical movement of the freshwater can be neglected. The Ghyben-Herzberg relationship uses a hydrostatic balance to show that the saltwater-freshwater interface is located at a depth below sea level approximately forty times that of the corresponding height of freshwater above sea level. Specifically, the relation is developed that

$$h_s = \frac{1}{\frac{\rho_s}{\rho_f} - 1} h_f \tag{2.1}$$

in which

h_f = height of fresh water above sea level

h_s = depth of salt-fresh interface below sea level

ρ_s, ρ_f = density of salt and freshwater, respectively

Since the density of sea water is typically about 1.025 times that of freshwater, Equation 2.1 suggests $h_s \approx 40h_f$. This also leads to the conclusion that decreasing the fresh water head by a unit value causes a resulting salt water interface rise of about 40 units.

Hubbert [1940], among others, has shown that where streamline curvature is pronounced, Equation 2.1 gives values somewhat in error; however, the Ghyben-Herzberg relation still provides a useful point of reference.

The actual change from fresh to saltwater occurs through a transition zone of varying density and salt concentration. Bear [1979] notes that the extent of the transition zone is dependent on local conditions. He shows data from Kohout [1960] and Israel showing extensive and small transition zones, respectively. One expects that interfacial mixing and dispersion, existing in a given region, will determine the transition zone characteristics. These mixing features are in turn controlled by pumping rates, existing groundwater flows, and aquifer characteristics. As Bear [1979] notes, even when the assumption of a sharp interface is reasonably valid, a transition zone exists.

If the scale of the overlying freshwater lens is large with respect to the transition zone, it may be reasonable to assume that there is a sharp interface separating the fresh and saltwater. Studies along this line were done by Hantush [1968] and Dagan and Bear [1968].

Bear [1979] summarizes these and other sharp-interface approximations. Strack [1976] utilized a single harmonic potential to define interface movement inland due to pumping. Many sharp interface studies attempt only two-dimensional approaches, simulating a line of wells parallel to the coast. Only a few deal with the three-dimensional field around single wells or overlapping fields of wells. As an example, Muskat [1937] presented a model attempting to account for partial penetration of a pumping well by superposition of sinks.

Using the sharp interface assumption, potential flow theory can be applied to both sides of the sharp interface between the fresh and saltwater, thus simplifying the calculation. However, in such calculations, salinity dispersion is neglected, and there is no direct method of estimating its effect on the dynamics (i.e. non-potential flow) of the flow and salinity distribution.

In more recent studies the effects of salinity dispersion at the interface are accounted for. Dagan [1971] formulated the equation of dispersion for a neutrally buoyant tracer in a steady flow by applying a coordinate system based on the potential and the stream function

[Bachmat and Bear, 1964]. Then, by applying singular perturbations as suggested by Wooding [1963; 1964] they analyzed the migration of a tracer being initially tangent or nontangent to a streamline. In a later study Eldor and Dagan [1972] extended the analysis to include radioactive decay and absorption.

Gelhar and Collins [1971] applied a boundary layer approximation to develop general solutions for one-dimensional problems involving longitudinal despersion of neutrally buoyant tracers in porous media.

Koh [1964] and List [1965; 1968] analyzed the problem of flow induced by axially symmetric and two-dimensional sinks in a stratified flow through a porous medium. They showed that boundary layer approximations can be applied for the simulation of flow conditions in the aquifer.

Rubin and Pinder [1977], utilizing a perturbation technique, studied the effect of salinity dispersion on the dynamics of groundwater flow as well as on the salinity distribution in a porous medium. The phenomenon is described as a migration of a sharp interface perturbed by small disturbances due to salinity dispersion. The creation of the mixing zone between fresh and saline water is described as a formation of a boundary layer in the vicinity of a sharp interface. This method is primarily recommended for flow fields in which simple representation of the sharp interface migration is obtainable. This model was modified to form the basis for calculation of indices indicating sensitivity to potential saltwater intrusion by Calderon [1981].

2.4 Numerical Studies

Simulations of flow conditions in an aquifer subject to density stratification due to salinity distribution can be done by applying complete numerical schemes for the performance of the simultaneous solution of the equations of motion and salinity transport.

Numerical techniques have an advantage over analytical techniques since they are able to handle complex boundary conditions, varying aquifer thicknesses, heterogeneous and anisotropic permeabilities, varying pumping rates, multiple wells, and recharge. However, such numerical flexibility requires substantially better field data for input and verification. Finite difference , finite element, and boundary element techniques have been used. Each has some limitations. For example, the finite difference solution is a numerical technique that uses a linear approximation of the differential terms in an equation. As a result, problems arise with stability and convergence to a solution in actual non-linear phenomena such as the stratified flow situation. Considering leaky aquifers, variability of the aquifer's permeability and that of the semiconfining formations leads to a significant increase in the grid size for regions in which the flow is very slow. Incorporation of multiple aquifers and aquicludes in a three-dimensional model cannot be practically done by the application of a complete numerical scheme. Problems of numerical dispersion stemming from the use of the finite grid size must also be considered. These problems can be minimized by various methods, but they cannot be avoided in complete numerical models.

A numerical approach was applied by Pinder and Cooper [1970], who developed a two-dimensional model based on a finite difference characteristic method for the simulation of the movement of a saltwater front in an aquifer. For the same purpose Segol et al. [1975] developed a finite element procedure that provides a complete solution of the two-dimensional equations of motion and salinity transport.

Christensen [1978] presented a finite element method for analysis of freshwater lenses in the coastal zones of the Floridan Aquifer. This was applied to a large area in Pinellas County but with no data available then for verification. It was based on assumption of no buoyant forces or dispersion, with a piston-type displacement of salt water by injected fresh water.

Rubin and Christensen [1982] and Rubin [1982] extended the integral approach to the simulation of unsteady state flow conditions in a two-dimensional aquifer subject to mineralization. Both studies use the integral boundary layer method whereby the solute transport equation is integrated over the vertical thickness of the transition zone subject to certain similarity conditions. The resulting equation is then solved simultaneously with the equations of continuity and motion by a finite difference scheme. This approach was extended by Means [1982] for the simulation of initial stages of saltwater intrusion in a three-dimensional flow field. Rubin and Benedict [1982a; 1982b] developed a two-dimensional procedure that can be used for the simulation of advanced stages of saltwater intrusion.

Wheatcraft and Peterson [1979] used a finite difference scheme to create a two-dimensional model simulating movement of a treated sewage due to injection in a saline aquifer.

Merritt [1983], in a joint United States Geological Survey and United States Corp of Engineers Project, studied the feasibility of recovering freshwater injected and stored underground in South Florida. An attempt was made to use the subsurface finite-difference waste disposal model [INTERCOMP 1976] to simulate the cyclic injection required by the injection-recovery project.

2.5 Summary

While analytical models are easy to apply and give solutions to simple aquifer situations, they have the disadvantage of not being able to accurately simulate complex flow phenomena. Numerical models can simulate complex flow phenomena but encounter problems with stability and convergence. Also, numerical models have large memory requirements and use considerable amounts of computer time, making them inaccessible to many professionals.

To overcome problems with stability, convergence, and computer requirements associated with numerical models, it may be necessary to make some simplifying assumptions, or even combine the model with analytical techniques.

CHAPTER 3

REVIEW OF PREVIOUS WORK

3.1 Introduction

Simulation of flow conditions in a saline aquifer subject to the injection of freshwater can be done by solving simultaneously the equations of continuity, motion, and solute transport. However, this procedure leads to a set of highly non-linear equations, thus causing problems with stability and convergence in a numerical solution.

By extending Rubin's [Rubin 1982] work, Means [1982] used an integral boundary layer technique whereby the solute transport equation was integrated over the vertical thickness of the transition zone subject to certain similarity conditions. By integrating through the transition zone, equations describing flow in that area were greatly simplified, thus making a numerical solution possible.

It is the intent of this report to modify the equations and extend the theory of the Means report in an effort to simulate the injection situation.

Before developing the equations to be used in the injection situation, it will first be helpful to briefly review the saltwater intrusion simulation done by Means.

3.2 The Approximate Method of Stratification Analysis

Figure 3.1 describes the typical flow field for the upconing situation in an inland aquifer. According to the figure, the flow field is divided into the following three zones:

(a) the upper zone of freshwater,

(b) the transition zone,

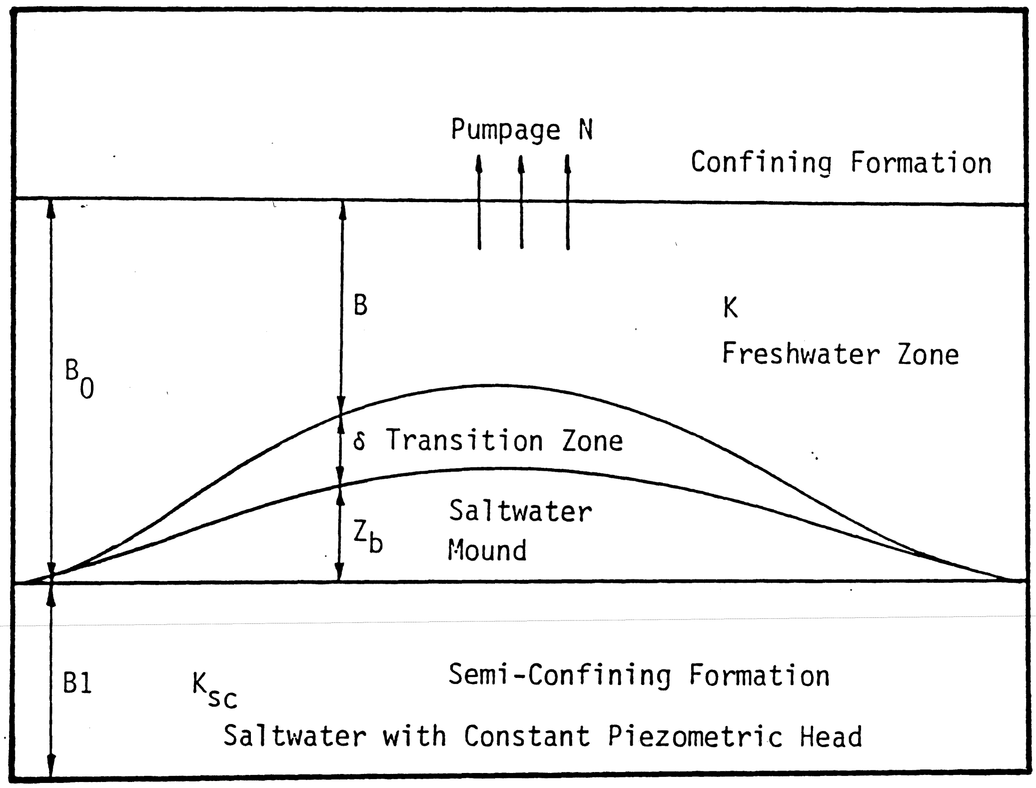

Figure 3.1 Schematic description of the development of a transition zone due to pumpage

(c) the underlying saltwater zone.

The flow in the freshwater zone is assumed to be horizontal and potential. Flow in the transition zone is assumed horizontal and non-potential. Displacement in the saltwater zone is assumed horizontal and non-potential. Displacement in the saltwater zone is assumed vertical and potential.

The basic equations used for the simulation of stratified flow in an aquifer are the equations of continuity, motion, solute transport, and state represented respectively as follows:

$$\nabla \cdot \vec{q} + \frac{\partial n}{\partial t} = 0 \tag{3.1}$$

$$\vec{q} = -\vec{K} \cdot \nabla\phi \tag{3.2}$$

$$n \frac{\partial C}{\partial t} + \nabla \cdot (\vec{q}C) = \nabla \cdot (\tilde{D} \cdot \nabla C) \tag{3.3}$$

$$\gamma = \gamma_o \ (1 + \alpha C) \tag{3.4}$$

in which

$\vec{q}$ = specific discharge vector

n = porosity

t = time

$\vec{K}$ = hydraulic conductivity

ϕ = hydraulic head

C = mineral concentration

$\tilde{D}$ = dispersion tensor

γ = unit weight

γ_o = unit weight of reference

α = constant relating mineral concentration with unit weight

3.3 The Integral Method of Boundary Layer Approximation

The integral method was applied to the problem of description of fluid boundary layers adjacent to solid boundaries. This method simplifies the appropriate equations by integrating over the boundary layer thickness. This procedure has been extended to many other types of problems in which integration occurs over some physical region of interest. Due to its original applications, this is often called a boundary layer approximation. This method has been widely used in treatment of the flow of jets and plumes in stratified or unstratified media.

In the integral method, one assumes mathematical forms for the profiles of parameters of interest, such as velocity and concentration, across the "boundary layer." The profiles are called similar profiles because the mathematical form is the same at each section, and some writers refer to these as similarity techniques. Once a similarity profile is introduced, this is the same as specifying the solution form within the "boundary layer" region. The integration of the basic equation, with these similarity profiles included, effectively reduces the dimensionality of the problem being solved. For example, in a circular jet discharge, specification of axisymmetric similar profiles and subsequent integration reduces the three-dimensional problem to one-dimensional.

As noted by Morton [1961] and Benedict, et al. [1974], the effect of assuming similar profiles is to suppress analytical solution of the details of the structure through the "boundary layer." Therefore, any reasonable profile could be assumed. While different assumed profiles might lead, for example, to different values for various empirical parameters, the prediction of the overall behavior of the phenomenon being modeled is presumed not highly sensitive to the form of profile chosen. However, if one is interested in using the profile form to predict concentrations or velocities at specific points in the flow field, then the form needs to be selected as accurately as possible. It should further be noted that any such integral approach decreases in accuracy as regions are reached where the assumption of similar profiles breaks down.

By integrating equations (3.2) and (3.3) through the transition zone and solving simultaneously equations (3.1), (3.2), (3.3) and (3.4), Means [1982] obtained a simplified description of the stratified flow situation. In the solution, two different polynomials were used for variation of salt concentration and specific discharge across the transition zone. The constraints were essentially the following:

(a) For concentration - salt water at the bottom of the transition zone, freshwater (zero concentration) at the top.

(b) For specific discharge in the horizontal direction - zero at the bottom of the transition zone, with the velocity from the freshwater region at the top of the transition zone.

The integration yields three equations with three unkowns: s, (drawdown), z_b (bottom of the transition zone), and δ (thickness of the transition zone). These equations are solved by an iterative ADI (Alternating Direction Implicit) finite difference scheme. The iteration is necessary because of the nonlinearity of the equations. Some features of the solution procedure will be useful to this work, but others will need substantial reworking. For example, some apparent anomalies exist in transition zone thickness beneath the center of the large pumping region studied by Means [1982]. These would be significant for a single well, as in the injection problem.

CHAPTER 4

ANALYSIS OF INJECTION

4.1 Introduction

In this chapter, equations (3.1), (3.2), (3.3), and (3.4) will be applied to the injection situation.

Figure 4.1 shows a profile of the injection situation. The flow field in a situation where freshwater is injected into a saline aquifer is the reverse of the flow field caused by upconing of saltwater under a pumping well. Instead of flow moving radially in toward the well, flow is now moving radially outward away from the well. Instead of having a saltwater mound under a pumping well, there is now a freshwater lens underneath an injection well.

The flow in the freshwater lens is assumed horizontal and potential; flow in the transition zone is assumed horizontal and non-potential; and flow in the saline region is assumed vertical and potential.

4.2 Development of Equations

The equation of motion vector (3.2) can be written in the vertical direction as

$$\vec{q}_z = -\vec{K}_z \cdot \frac{\partial \phi}{\partial z} \tag{4.1}$$

where

$$\phi = \frac{p}{\gamma} + z \tag{4.2}$$

Inserting (4.2) into (4.1), multiplying by γ and dividing by $\vec{K}$ yields

$$\frac{q_z \gamma}{\vec{K}_z} = \frac{\partial p}{\partial z} + \gamma \tag{4.3}$$

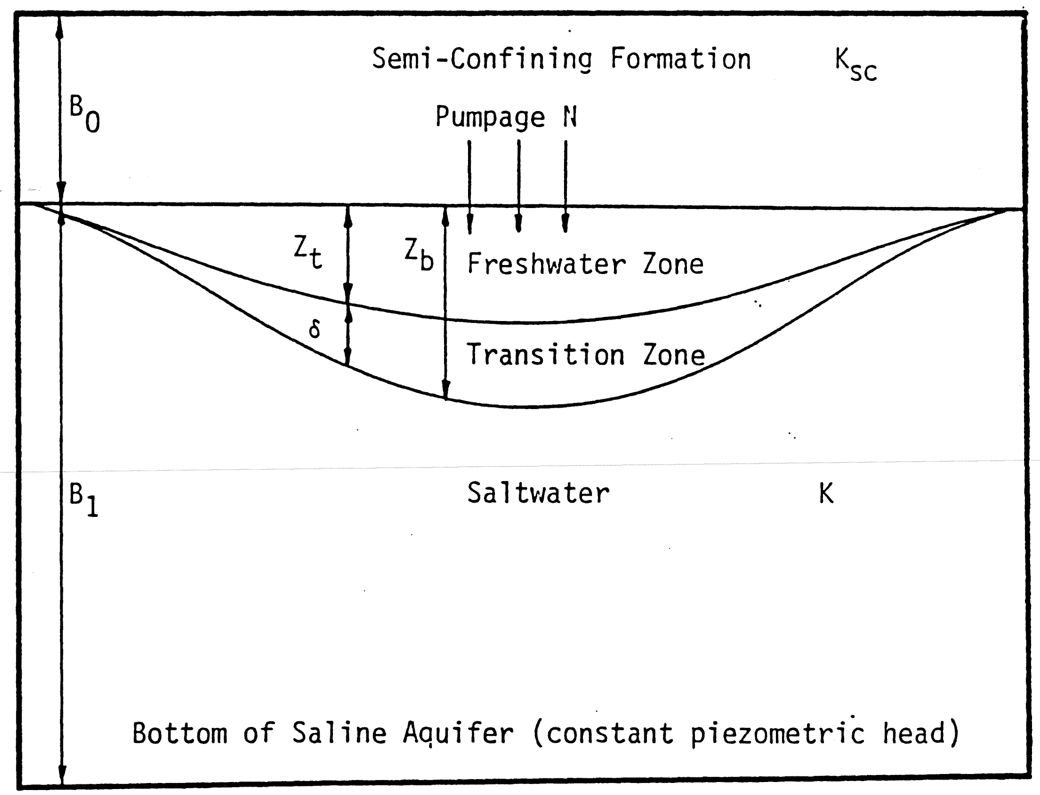

Figure 4.1 Schematic description of the development of a transition zone due to a freshwater injection into a saline aquifer

by assuming that flow in the transition zone is horizontal ($\vec{q}_z = 0$) yields

$$\partial p = -\gamma dz \tag{4.4}$$

Integrating (4.4) through the vertical thickness of the transition zone yields

$$P_t - P_b = - \int_{-z_b}^{-z_t} \gamma dz \tag{4.5}$$

where indices t and b represent the top and bottom of the transition zone, respectively. Applying (4.2) to fresh and saline water results in

$$\phi_{ft} = \frac{P_t}{\gamma_f} - z_t \tag{4.6a}$$

$$\phi_{sb} = \frac{P_b}{\gamma_s} - z_b \tag{4.6b}$$

where indices f and s represent fresh and saline water, respectively. Rearranging (4.6a) and (4.6b)

$$P_t = \gamma_f(\phi_{ft} + z_t) \tag{4.7a}$$

$$P_b = \gamma_s(\phi_{sb} + z_b) \tag{4.7b}$$

substituting (4.7a) and (4.7b) into (4.5), and dividing by $-\gamma_o$ yields

$$\frac{\gamma_s}{\gamma_o}(\phi_{sb} + z_b) - \frac{\gamma_f}{\gamma_o}(\phi_{ft} + z_t) = \int_{-z_b}^{-z_t} \frac{\gamma}{\gamma_o} dz \tag{4.8}$$

From (3.4) it can be seen that

$$\gamma_s = \gamma_o(1 + \alpha C_s) \tag{4.9a}$$

$$\gamma_f = \gamma_o(1 + \alpha C_f) \tag{4.9b}$$

Inserting (3.4), (4.9a) and (4.9b) into (4.8)

$$\frac{\gamma_o}{\gamma_o}(1 + \alpha C_s)(\phi_{sb} + z_b) - \frac{\gamma_o}{\gamma_o}(1 + \alpha C_f)(\phi_{ft} + z_t)$$

$$= \int_{-z_b}^{-z_t} \frac{\gamma_o}{\gamma_o}(1 + \alpha C)dz \tag{4.10}$$

It is assumed that the transition zone is a boundary layer where the specific discharge and the solute concentration profiles satisfy the following similarity conditions

$$u = UF(\eta) \tag{4.11a}$$

$$v = VF(\eta) \tag{4.11b}$$

$$C = C_oL(\eta) \tag{4.11c}$$

where u and v are the components of specific discharge in the horizontal x and y direction, respectively; U and V are the characteristic specific discharge in the horizontal x and y direction, respectively: C_o is the characteristic concentration: F and L are the distribution functions for specific discharge and solute concentration, respectively; η is the dimensionless coordinate within the transition zone and is defined as

$$\eta = \frac{[z - (-z_b)]}{\delta} = \frac{(z + z_b)}{\delta}\text{, and} \tag{4.12}$$

$$\delta = -z_t - (-z_b) = z_b - z_t \tag{4.13}$$

where, δ is the thickness of the transition zone. Integrating (4.12)

$$\frac{\partial \eta}{\partial z} = \frac{1}{\delta} \tag{4.14}$$

Introducing (4.11c), (4.12), and (4.14) into (4.10)

$$(1 + \alpha C_s)(\phi_{sb} + z_b) - (1 + \alpha C_f)(\phi_{ft} + z_t)$$

$$= \int_0^1 [1 + \alpha C_oL(\eta)]\delta d\eta \tag{4.15}$$

By introducing (4.13) into (4.15), cancelling δ on both sides of the equation and rearranging

$$(1 + \alpha C_s)\,\phi_{sb} - (1 + \alpha C_f)\phi_{ft} + \alpha C_f \delta + \alpha(C_s - C_f)z_b$$
$$= \alpha C_o \delta \int_0^1 L(n)dn \qquad (4.16)$$

Defining the salt concentration in freshwater, C_f as $C_f = 0$, and saline water, C_s as $C_s = C_o$ and rearranging (4.16)

$$\phi_{ft} = (1 + \xi)\phi_{sb} + \xi Z_b - \xi\delta \int_0^1 L(n)dn \qquad (4.18a)$$

where

$$\xi = \alpha C_o = (\gamma_s - \gamma_f)/\gamma_f \qquad (4.18b)$$

It is assumed that only constant vertical flow exists in the saltwater below the transition zone; as a result, (3.1) becomes

$$\frac{\partial w}{\partial z} = 0 \qquad (4.19)$$

where w is the vertical velocity that does not vary vertically, and is therefore equal to the value it attains at the bottom of the transition zone, which is given by

$$\frac{\partial(-z_b)}{\partial t} = \frac{q_z}{n} = -\frac{\vec{K}_z}{n}\frac{\partial\phi}{\partial z} \qquad (4.20)$$

The negative sign in the term on the left side of (4.20) is used since it is known that the freshwater lens is growing in the negative direction, and one is interested only in the magnitude of the term. Rearranging and integrating through the saltwater region

$$\int_{-Bl}^{-zb} \partial\phi = n\,\frac{\partial z_b}{\partial t} \int_{-Bl}^{-zb} \frac{\partial z}{K} \qquad (4.21)$$

Carrying out the integration, (4.21) becomes

$$\phi_b - \phi_{B1} = n \frac{\partial z_b}{\partial t} \left[\frac{-z_b + B1}{K}\right] \tag{4.22}$$

Initially, $\phi_{B1} = \phi_{so}$, where ϕ_{so} is the piezometric head at the bottom of the aquifer substituting for ϕ_{B1} and rearranging (4.22).

$$\phi_{sb} = \phi_{so} + n \frac{\partial z_b}{\partial t} \left[\frac{B1 - z_b}{K}\right] \tag{4.23}$$

It is assumed that before injection occurs, vertical equipotentials exist throughout the aquifer, whereby applying continuity of pressure gives

$$\phi_{so}\gamma_s = \phi_{fo}\gamma_f \tag{4.23b}$$

Introducing (4.23) and (4.23b) into (4.18) gives

$$\phi_{ft} = \phi_{fo} + (1 + \xi)n \frac{\partial z_b}{\partial t} \left[\frac{B1 - z_b}{K}\right] + \xi z_b$$

$$- \xi\delta \int_0^1 L(n)dn \tag{4.24}$$

The increase of potentiometric head at a point due to injection into an aquifer is defined as

$$s = \phi_{ft} - \phi_{fo} \tag{4.25}$$

where s is the head build-up. Introducing (4.25) into (4.24) and rearranging yields

$$\frac{\partial z_b}{\partial t} = \frac{K}{n(B1 - z_b)(1 + \xi)} \left(s - \xi z_b + \xi\delta \int_0^1 L(n)dn\right) \tag{4.26}$$

which is the equation describing the rate of growth of the freshwater lens.

The continuity equation (3.1) will be used for the derivation of the equation that will describe the increase in potentiometric head due to injecting freshwater into a saline aquifer. Equation (3.1) can be written in the following form

$$\frac{\partial}{\partial x}(q_x) + \frac{\partial}{\partial x}(q_y) + \frac{\partial}{\partial z}(q_z) = -S\frac{\partial s}{\partial t} \tag{4.27}$$

where S is the storativity of the aquifer. The sign of the right hand side of Equation (4.27) is consistent with the definition of s in Equation (4.25). Integrating (4.27) vertically from the bottom of the transition zone to the top of the freshwater zone

$$\frac{\partial}{\partial x}\int q_x dx + \frac{\partial}{\partial y}\int q_y dz + \int \partial(q_z) = -S\frac{\partial s}{\partial t} \tag{4.28}$$

It has been stated in equations (4.11a) and (4.11b) that

$$q_x = u = UF(n) \tag{4.29a}$$

$$q_y = v = VF(n) \tag{4.29b}$$

Introducing (4.29a) and (4.29b) into (4.28)

$$\begin{aligned}\frac{\partial}{\partial x}\Big[\int_{-z_b}^{-z_t} U\,F(n)dz + \int_{-z_t}^{0} U\,dz + \int_{0}^{BO} U_1 dz\Big]\\ + \frac{\partial}{\partial y}\Big[\int_{-z_b}^{-z_t} V\,F(n)dz + \int_{-z_t}^{0} V\,dz + \int_{0}^{BO} V_1 dz\Big]\\ + \int_{-z_b}^{0}\partial(q_z) + \int_{0}^{BO}\partial q_z = -S\frac{\partial s}{\partial t}\end{aligned} \tag{4.30}$$

where $\int_{0}^{BO} \partial q_z = 0$ since flow is horizontal. It can be seen from (3.2) that

$$U = - K \frac{\partial s}{\partial x} \tag{4.31a}$$

$$V = - K \frac{\partial s}{\partial y} \tag{4.31b}$$

Once again, the sign of the derivatives is consistent with the definition of s given in Equation (4.25). U_1 and V_1 are the horizontal velocities in the semi-confining layer. Introducing (4.31a) and (4.31b) into (4.30) and integrating yields

$$- \frac{\partial}{\partial x} [\int_{-z_b}^{-z_t} K \frac{\partial s}{\partial x} F(n)\, dz + \int_{-z_t}^{0} K \frac{\partial s}{\partial x}\, dz + \int_{0}^{BO} K_{sc} \frac{\partial s}{\partial x}\, dz]$$

$$- \frac{\partial}{\partial y} [\int_{-z_b}^{-z_t} K \frac{\partial s}{\partial y} F(n)\, dz + \int_{-z_t}^{0} K \frac{\partial s}{\partial y}\, dz + \int_{0}^{BO} K_{sc} \frac{\partial s}{\partial y}\, dz]$$

$$+ q_{z.0} - q_{z.z_b} = - S \frac{\partial s}{\partial t} \tag{4.32}$$

where

K_{sc} = permeability of the semi-confining layer

$q_{z.0}$ = vertical specific discharge at the top of the confining layer which is equal to the pumping velocity, -N.

$q_{z.z_b}$ = $-n \frac{\partial z_b}{\partial t}$, the "specific discharge" of the freshwater lens.

Substituting for $q_{z.0}$ and $q_{z.zb}$, and introducing (4.12) and (4.14) into (4.32)

$$\frac{\partial}{\partial x} [K(\beta + \delta \int_{0}^{1} F(n)dn) \frac{\partial s}{\partial x}] + \frac{\partial}{\partial y} [K(\beta + \delta \int_{0}^{1} F(n)dn) \frac{\partial s}{\partial y}]$$

$$+ N - n \frac{\partial z_b}{\partial t} = S \frac{\partial s}{\partial t} \tag{4.33}$$

where

$$\beta = \frac{BOK_{sc}}{K} + z_b - \delta \tag{4.34}$$

The development of the equation describing the growth of the transition zone involves application of conservation of mass of the constituent. Note that in Figure 4.2 it is assumed that all dispersed material comes from the saltwater region, and that no diffusion of the material occurs across the top of the transition zone. The rate of change of storage of the constituent in a given volume is equal to the sum of all inflows and outflows of the material, plus any internal sources and sinks (such as radioactive decay, biological degradation, etc., none of which exists for salt).

$$\sigma(t) = \int_{-z_b}^{-z_b+\delta} nC\ dz\ dx\ dy \tag{4.35a}$$

$$\sigma(t + \Delta t) = \int_{-z_b}^{-z_b+\delta} nC\ dz\ dx\ dy + \frac{\partial}{\partial t}\left[\int_{-z_b}^{-z_b+\delta} nC\ dz\ dx\ dy\right]\Delta t \tag{4.35b}$$

where $\sigma(t)$ is the original storage and $\sigma(t + \Delta t)$ is the storage at time $t + \Delta t$.

The difference between (4.35a) and (4.35b) is

$$\Delta\sigma = \frac{\partial}{\partial t}\left(\int_{-z_b}^{-z_b+\delta} nC\ dz\ dx\ dy\right)\Delta t \tag{4.36}$$

The inflows by convection are

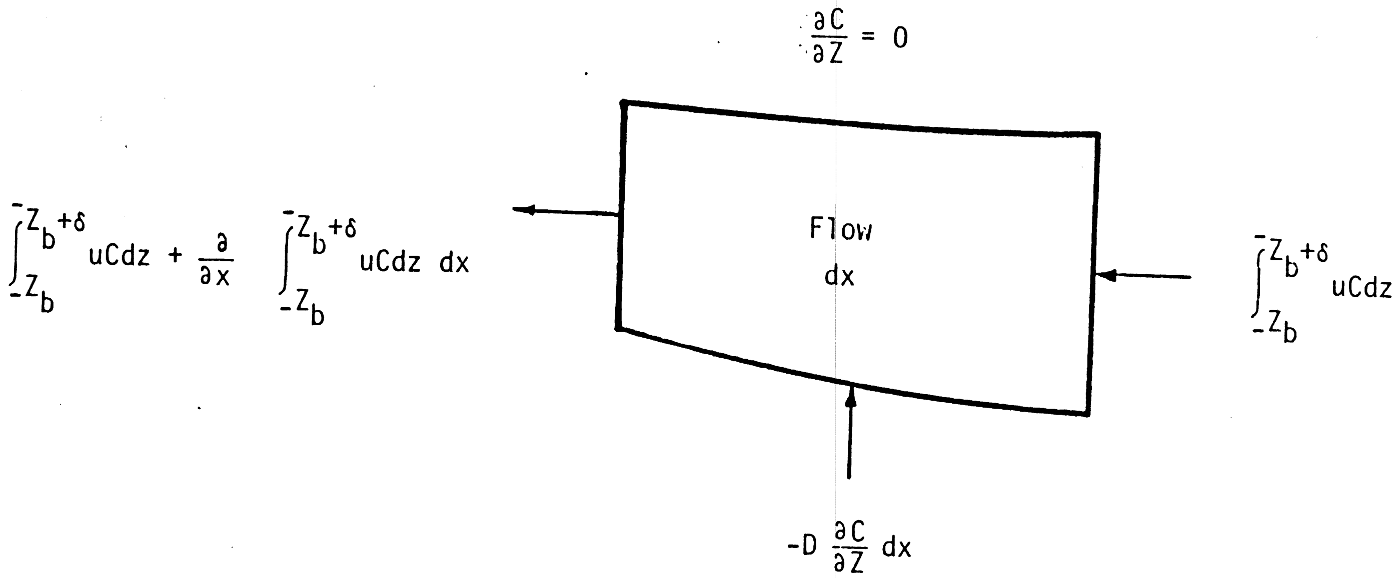

Figure 4.2 Control volume for the development of Equation 4.47

$$\Delta\kappa = \int_{-z_b}^{-z_b+\delta} nC\ dzdxdy - [\int_{-z_b}^{-z_b+\delta} uC\ dzdy + \frac{\partial}{\partial x}(\int_{-z_b}^{-z_b+\delta} dzdy)\Delta x]$$
$$+ \int_{-z_b}^{-z_b+\delta} vC\ dzdx - [\int_{-z_b}^{-z_b+\delta} uC\ dzdy$$
$$+ \frac{\partial}{\partial y}(\int_{-z_b}^{-z_b+\delta} vC\ dzdx)\Delta y] \qquad (4.37)$$

where $\Delta\kappa$ is the solute inflow due to convection. Simplifying (4.37)

$$\Delta\kappa = -\frac{\partial}{\partial x}\int_{-z_b}^{-z_b+\delta} uC\ dzdydx - \frac{\partial}{\partial y}\int_{-z_b}^{-z_b+\delta} vC\ dzdxdy \qquad (4.38)$$

Dispersion is assumed to only occur vertically

$$\Psi_{in} = -(D\frac{\partial C}{\partial z})dxdy \qquad (4.39a)$$

$$\Psi_{out} = 0 \qquad (4.39b)$$

where Ψ_{in} is the dispersion flow into the control volume; Ψ_{out} is the flow out of the control volume, which is zero; and D is the dispersion coeficient.

Since the change in storage in the control volume is equal to the net inflows and outflows of the material

$$\Delta\sigma = \Delta\kappa + \Psi_{in} - \Psi_{out} \qquad (4.40)$$

Substituting (4.36), (4.38), (4.39a) and (4.39b) into (4.40) and multiplying $\Delta\kappa$ and Ψ by Δt yields

$$\frac{\partial}{\partial t}\left(\int_{-z_b}^{-z_b+\delta} nC\ dzdxdy\right)\Delta t = -\left(\frac{\partial}{\partial x}\int_{-z_b}^{-z_b+\delta} uC\ dzdydx\right)\Delta t$$

$$-\frac{\partial}{\partial y}\left(\int_{-zb}^{-zb+\delta} vC\ dzdxdy\right)\Delta t - D\frac{\partial C}{\partial z}\Big/_{-zb} dxdy\Delta t \qquad (4.41)$$

Introducing (4.12), (4.14), (4.11a), (4.11b), and (4.11c) into (4.41), and integrating with respect to z and dividing by dxdy

$$\frac{\partial}{\partial t}\int_0^1 n\delta C_o L(n)dn + \frac{\partial}{\partial x}\int_0^1 \delta UF(n)C_o L(n)dn$$

$$+\frac{\partial}{\partial y}\int_0^1 \delta VF(n)C_o L(n)dn = -D\,\frac{\partial C_o L(n)}{\delta\,\partial n}\Big/_{n=0} \qquad (4.42)$$

Note that

$$\delta\,\frac{\partial\delta}{\partial t} = \frac{1}{2}\,\frac{\partial\delta^2}{\partial t} \qquad (4.43a)$$

$$\delta\,\frac{\partial\delta}{\partial x} = \frac{1}{2}\,\frac{\partial\delta^2}{\partial x} \qquad (4.43b)$$

$$\delta\,\frac{\partial\delta}{\partial y} = \frac{1}{2}\,\frac{\partial\delta^2}{\partial y} \qquad (4.43c)$$

Further

$$\delta\,\frac{\partial}{\partial x}\,\delta U = \delta\left[\delta\,\frac{\partial U}{\partial x} + U\,\frac{\partial\delta}{\partial x}\right] = \delta^2\,\frac{\partial U}{\partial x} + \frac{U}{2}\,\frac{\partial\delta^2}{\partial x} \qquad (4.44a)$$

Similarly

$$\delta\,\frac{\partial}{\partial y}\,\delta V = \delta\left[\delta\,\frac{\partial V}{\partial y} + V\,\frac{\partial\delta}{\partial x}\right] = \delta^2\,\frac{\partial V}{\partial y} + \frac{V}{2}\,\frac{\partial\delta^2}{\partial y} \qquad (4.44b)$$

Multiplying by δ, dividing by C_0, and introducing (4.43a), (4.35b), (4.43c), (4.44a) and (4.44b), equation 4.42 becomes

$$\left(\frac{n}{2}\int_0^1 L(n)dn\right)\frac{\partial\delta^2}{\partial t} + \left[\delta^2\left(\frac{\partial U}{\partial x}+\frac{\partial V}{\partial y}\right)\right.$$

$$\left. + \frac{1}{2}\left(U\frac{\partial\delta^2}{\partial x} + V\frac{\partial\delta^2}{\partial y}\right)\right]\int_0^1 F(n)\,L(n)\,dn = -DL'(0) \qquad (4.45)$$

Where D is generally accepted to be equal to the absolute value of the specific discharge

$$D = a\,(U^2+V^2)^{1/2} \qquad (4.46)$$

where a is equal to the transverse dispersivity of the aquifer.

Introducing Equations (4.46), (4.31a) and (4.31b) into (4.45)

$$\left(\frac{n}{2}\int_0^1 L(n)dn\right)\frac{\partial\delta^2}{\partial t} - \left[\delta^2 K\left(\frac{\partial^2 s}{\partial x^2}+\frac{\partial^2 s}{\partial y^2}\right) + \frac{1}{2}K\left(\frac{\partial s}{\partial x}\frac{\partial\delta}{\partial x} + \frac{\partial s}{\partial y}\frac{\partial\delta^2}{\partial y}\right)\right]$$

$$\int_0^1 F(n)\,L(n)\,dn = -\,a\,K\left[\left(-\frac{\partial s}{\partial x}\right) + \left(-\frac{\partial s}{\partial y}\right)^2\right]^{1/2} L'(0) \qquad (4.47)$$

The pertinent equations to solve now become Equations (4.26), (4.33), (4.34) and (4.47). These equations could be solved by perturbation techniques (e.g. Rubin and Pinder, 1977), but the possibilities of multiple wells and aquifer inhomogeneities suggest that a numerical solution will provide more flexibility. Such a solution procedure will be outlined in Chapter 5.

The equations developed in this chapter should provide a sound basis for analysis of many injection problems. Numerous assumptions have been made to simplify the equations while still maintaining the basic character of the physical system.

CHAPTER 5

NUMERICAL SIMULATION

5.1 Development of the Numerical Model

Equations (4.26), (4.33) and (4.47) completely describe the flow process due to a freshwater injection into a saline aquifer. Equation (4.34) allows continuous updating of the flow thickness. In this chapter a method will be devised in which these equations can be solved simultaneously to provide a description of the injection process. Since equations (4.26), (4.33) and (4.47) are non-linear and expressed by three independent variables (two spatial variables and a time variable), a numerical scheme will provide the most direct solution. Since finite element and boundary integral models are generally more site-specific and useful for only one application, a finite difference numerical scheme will be used. The finite difference scheme has the advantage of being applicable to a wide variety of boundary situations, requiring somewhat less input data, and requiring somewhat less computer time and space.

Since equations (4.26), (4.33) and (4.47) must all be solved simultaneously, it is advantageous to use an iterative alternating direction implicit (IADI) finite difference method. The main advantage of using an ADI method is that for each time step it reduces large sets of simultaneous equations into smaller sets [Bear, 1979]. The ADI method is accomplished by breaking the desired forward stepping in time into two steps. First, the unknowns are solved for in the x-direction at the advanced time step using the known terms being set in the y-direction at the previous time step. In the second half advancing time step, the situation reverses. The unknown values at the advanced time step are now written in the y-direction and are solved using the values in the x-direction at the previous time step. Since equations (4.26), (4.33) and (4.47) are all interdependent on each other, it is necessary to solve them iteratively. This means that the ADI process is repeated for each time step, using in each iteration updated values.

5.1.1 A Finite Difference Approximation of Equation (4.33)

In formulating a finite difference approximation for equation (4.33), an ADI method is used so that there are only three unkown variables at one node (the three variables at the advanced time step). Using only three unknowns at each node, a tridiagonal matrix can be generated for each column or row of a time step. This is the main reason for going to an ADI method, for reduction to a tridiagonal matrix allows use of the highly efficient Thomas algorithm for solution of the system of equations.

An implicit ADI finite difference scheme for the calculation of head build up, (4.33), is presented as follows:

First, the calculations are made for the unknowns in the x-direction at the (m+1) time step using known values in the y-direction at the (m) level.

$$s_{i-1,j}^{(m+1)}\left[\left(\beta + \delta \int_0^1 F(n)dn\right) \frac{K\Delta t}{(\Delta x)^2}\right]_{i-0.5,j}^{(m+0.5)} + s_{i,j}^{(m+1)} \Big\{S + \left[\left(\beta + \delta \int_0^1 F(n)dn\right) \frac{k\Delta t}{(\Delta x)^2}\right]_{i+0.5,j}^{(m+0.5)} + \left[\left(\beta + \delta \int_0^1 F(n)dn\right) \frac{k\Delta t}{(\Delta x)^2}\right]_{i-0.5,j}^{(m+0.5)}\Big\}$$

$$-s_{i+1,j}^{(m+1)}\left[\left(\beta + \delta \int_0^1 F(n)dn\right)\frac{K\Delta t}{(\Delta x)^2}\right]_{i+0.5,j}^{(m+0.5)} = S\, s_{i,j}^{(m)} - n \left(\frac{\partial z_b}{\partial t}\right)_{i,j}^{(m+0.5)} \Delta t$$

$$+ N_{i,j}\ \Delta t + (s^{(m)}_{i,j+1} - s^{(m)}_{i,j})[(\beta + \delta \int_0^1 F(n)dn)\ \frac{K\Delta t}{(\Delta y)^2}]^{(m+0.5)}_{i,j+0.5}$$

$$+ (s^{(m)}_{i,j-1} - s^{(m)}_{i,j})[(\beta + \delta \int_0^1 F(n)dn)\ \frac{K\Delta t}{(\Delta y)^2}]^{(m+0.5)}_{i,j-0.5} \qquad (5.1)$$

where

$$\beta = \frac{BO\ K_{sc}}{K} + z_b - \delta \qquad (5.2)$$

In Equation (5.1), the notation m implies known values from the previous time step, while (m+0.5) represents an average over the time step from time (m) to time (m+1). Similarly, the notation (i-0.5) and (i+0.5) implies use of appropriate average values over the space increment from i-1 to i and from i to i+1, respectively. The notation j+0.5 has a similar meaning. For example, the value of δ used in such averaged terms will be the average of the δ values at the two end points of the indicated region. Note that this also allows one to conveniently specify K values which vary spatially.

Next, the calculations are made for the unknowns in the y-direction at the (m+2) time step using the previously calculated values in the x-direction at the (m+1) time step.

$$-s^{(m+2)}_{i,j-1}\ [(\beta + \delta \int_0^1 F(n)dn)\frac{k\Delta t}{(\Delta y)^2}]^{(m+1.5)}_{i,j-0.5} + s^{(m+2)}_{i,j}\ \{S + [(\beta$$

$$+ \delta \int_0^1 F(n)dn)\ \frac{k\Delta t}{(\Delta y)^2}]^{(m+1.5)}_{i,j+0.5} + [(\beta + \delta \int_0^1 F(n)dn\frac{k\Delta t}{(\Delta y)^2}]^{(m+1.5)}_{i,j-0.5}\}$$

$$-s^{(m+2)}_{i,j+1}\ [(\beta + \delta \int_0^1 F(n)dn\ \frac{k\Delta t}{(\Delta y)^2}]^{(m+1.5)}_{i,j+0.5} = S\ s^{(m+1)}_{i,j}\ -n\ (\frac{\partial z_b}{\partial t})^{(m+1.5)}_{i,j}\Delta t$$

$$+ N_{i,j}\Delta t + (s^{(m+1)}_{i+1,j} - s^{(m+1)}_{i,j}[(\beta + \delta \int_0^1 F(n)dn)\frac{k\Delta t}{(\Delta x)^2}]^{(m+1.5)}_{i+0.5,j} + (s^{(m+1)}_{i-1,j}$$

$$- s_{i,j}^{(m+1)})[(\beta + \delta \int_0^1 F(n)dn)\frac{K\Delta t}{(\Delta x)^2}]_{i-0.5,j}^{(m+1.5)} \qquad (5.3)$$

where β is defined by (5.2)

In Equation (5.3), the 0.5 superscripts again mean averages over the pertinent temporal or spatial increment. The superscript (m+1.5) implies a time average over the step from (m+1) Δt to (m+2)Δt. The spatial subscripts such as (i+0.5), (i+0.5), and (j-0.5) represent spatial averages as in Equation 5.1.

5.1.2 <u>A Finite Difference Approximation to Equation (4.47)</u>

It was observed that when Means [1982] used a centered difference scheme for representation of the velocities in his pumping model, several anomalies occured in the vicinity of the well.

It is generally accepted that a centered difference scheme gives the most accurate finite difference description of gradients in the vicinity of a point. It has been observed in this report however, that the centered difference scheme does not work when representing velocities (head gradients) in the vicinity of a well. At a relative maximum or minimum on a head-curve, a centered difference scheme will give a gradient of zero. This is technically the correct gradient when Δx goes to zero, but for a finite grid size there actually is a relatively large gradient in the increment adjacent to the well. It is for this reason that a backward difference scheme is used when representing velocity terms in the transition zone thickness calculation. The following is a backward difference representation of the squared thickness of the transition zone in the x-direction:

$$\left(\frac{n}{2}\int_0^1 L(n)dn\right)\frac{\delta^{2(m+1)}_{i,j}-\delta^{2(m)}_{i,j}}{\Delta t}-\left[\delta^{2(m+1)}_{i,j}K_{i,j}\left(\frac{s^{(m+1)}_{i+1,j}-s^{(m+1)}_{i,j}+s^{(m+1)}_{i-1,j}}{(\Delta x)^2}\right)\right.$$

$$+\delta^{2(m)}_{i,j}K_{i,j}\left(\frac{s^{(m)}_{i,j+1}-s^{(m)}_{i,j}+s^{(m)}_{i,j-1}}{(\Delta y)^2}\right)+\frac{1}{2}K_{i,j}\left(\frac{s^{(m+1)}_{i,j}-s^{(m+1)}_{i-1,j}}{\Delta x}\right)$$

$$\left.\left(\frac{\delta^{2(m+1)}_{i,j}-\delta^{2(m+1)}_{i-1,j}}{\Delta x}\right)+\frac{1}{2}K_{i,j}\left(\frac{s^{(m)}_{i,j}-s^{(m)}_{i,j-1}}{\Delta y}\right)\left(\frac{\delta^{2(m)}_{i,j}-\delta^{2(m)}_{i,j-1}}{\Delta y}\right)\right]\int_0^1 F(n)L(n)dn$$

$$=-ak_{i,j}\left[\left(\frac{-s^{(m+1)}_{i,j}+s^{(m+1)}_{i-1,j}}{\Delta x}\right)^2+\left(\frac{-s^{(m+1)}_{i,j}+s^{(m+1)}_{i,j-1}}{\Delta y}\right)^2\right]^{1/2}\quad L'(0) \tag{5.4}$$

The equation can now be solved implicitly for $\delta^{2\,(m+1)}_{i,j}$.

Likewise, for the calculation of the squared thickness of the transition zone in the y-direction at time step (m+2), equation (4.47) can be written as follows:

$$\left(\frac{n}{2}\int_0^1 L(n)dn\right)\frac{\delta^{2(m+2)}_{i,j}-\delta^{2(m+1)}_{i,j}}{\Delta t}-\left[\delta^{2(m+1)}_{i,j}K_{i,j}\left(\frac{s^{(m+1)}_{i+1,j}-s^{(m+1)}_{i,j}+s^{(m+1)}_{i-1,j}}{(\Delta x)^2}\right)\right.$$

$$+\delta^{2(m+2)}_{i,j}K_{i,j}\left(\frac{s^{(m+2)}_{i,j+1}-s^{(m+2)}_{i,j}+s^{(m+2)}_{i,j-1}}{(\Delta y)^2}\right)+\frac{1}{2}K_{i,j}\left(\frac{s^{(m+1)}_{i,j}-s^{(m+1)}_{i-1,j}}{\Delta x}\right)$$

$$\left.\left(\frac{\delta^{2(m+1)}_{i,j}-\delta^{2(m+1)}_{i-1,j}}{\Delta x}\right)+\frac{1}{2}K_{i,j}\left(\frac{s^{(m+2)}_{i,j}-s^{(m+2)}_{i,j-1}}{\Delta y}\right)\left(\frac{\delta^{2\,(m+2)}_{i,j}-\delta^{2\,(m+2)}_{i,j-1}}{\Delta y}\right)\right]$$

$$\int_0^1 F(n)L(n)dn = -aK_{i,j}\left[\left(\frac{-s_{i,j}^{(m+1)} + s_{i-1,j}^{(m+1)}}{\Delta x}\right)^2 + \left(\frac{-s_{i,j}^{(m+2)} + s_{i,j-1}^{(m+2)}}{\Delta y}\right)^2\right]^{1/2} L'(0) \tag{5.5}$$

This equation can also be solved for $\delta^{2\,(m+1)}_{i,j}$

5.1.3 A Finite Difference Approximation to Equation (4.26)

The equation for calculation of the change in thickness of the freshwater lens with respect to time is written simply as follows:

$$\left(\frac{\partial z_b}{\partial t}\right)^{m+0.5}_{i,j} = \left[\frac{K}{n(B1-z_b)(1+\xi)}\left(s - \xi z_b + \xi\delta \int_0^1 L(n)dn\right]^{(m+0.5)}_{i,j} \tag{5.6}$$

5.1.4 General Solution Procedure

First a grid is created in the x-y plane. On the grid there are n number of nodes in the x-direction each spaced Δx distance apart. There are m number of nodes in the y-direction that are each spaced Δy distance apart. Arrays containing the permeabilities, storativities, and well magnitudes for each point are superimposed on the finite difference grid so that each point on the grid is represented by its corresponding points on the arrays.

As the solution procedure begins, the head buildups are first calculated using the ADI method. Depending on the time step, Equation (5.1) or (5.3) is used. At the first time step, Equation (5.1) is used going in the x-direction one row at a time. At the end of each row a tri-diagonal matrix has been formed and is solved using the Thomas Algorithm. After Equation (5.1) has been solved, the values of the head build-up will be used in the solution of the thickness of the transition zone, Equation (5.4).

With the values calculated in the head build-up and the transition zone thickness, the solution of the change in size of the freshwater lens with respect to time can be calculated from Equation (5.6). As stated previously, the solution of the governing equations must be iterative since the equations are nonlinear. The iterations continue until some specified level of tolerance is met; that is, the difference in the parameter from one iteration to the next must be less than the specified allowable difference.

Once the required tolerance has been met in the x-direction portion of the ADI prodecure, the next time step proceeds. Drawdowns are calculated using Equation (5.3), with δ^2 being obtained from Equation (5.5). The bottom of the transition zone can be found by use of Equation (5.6). Figure 5.1 shows a concise flow chart illustrating the calculation strategy.

5.2 Stability and Convergence Characteristics of Numerical Scheme

Because the equations being used here are nonlinear, it is difficult to perform one of the standard stability analyses on the equations to determine their expected stability and convergence as a function of time and distance steps and the pertinent physical parameters. However, some preliminary estimates can be made based on available literature on solution of the groundwater and diffusion equations by similar schemes. Bear (1979), Holly (1975), and numerous others present such material. The basic drawdown equation, Equation (4.33), with finite difference counterparts (5.1) and (5.3), should be influenced only slightly by values of δ and z_b. The stability criterion for it, as well as an indicator of convergence (or accuracy), should be something like

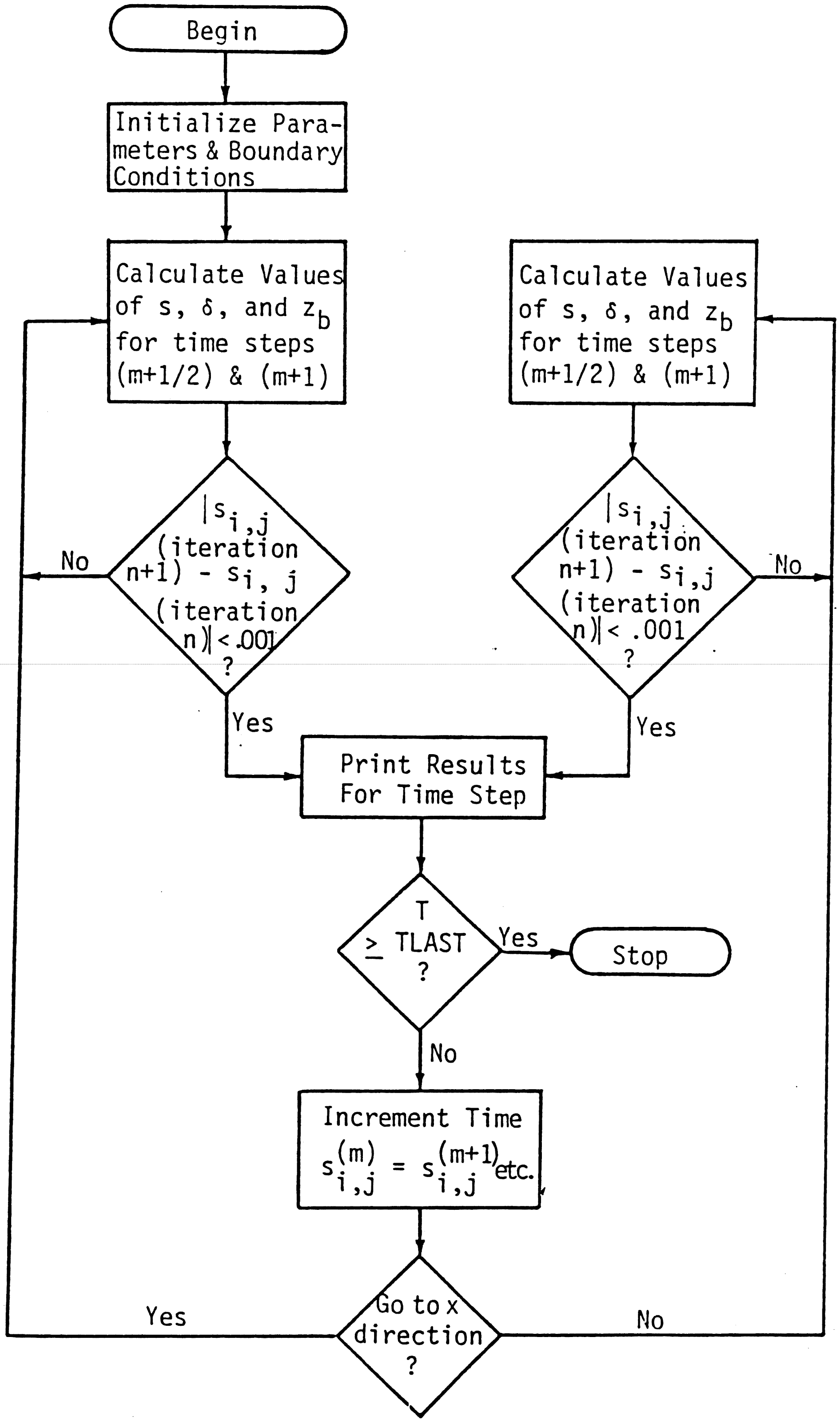

Figure 5.1 Flow Chart

$$\frac{T}{S}\frac{\Delta t}{\Delta x^2} \leq C_1 \tag{5.7}$$

in which C_1 = constant depending on the exact scheme used, but probably about 0.5.

Similarly, the dispersion equation, represented by Equation (4.47) and its finite difference representation Equation (5.4) or (5.5), will likely adhere to a constraint something like

$$D\frac{\Delta t}{\Delta x^2} \leq C_2 \tag{5.8}$$

in which C_2 = a constant which may or may not be equal to C_1.

There may be other constraints placed on model performance as well. For example, numerical experimentation suggested that for the very first time steps some relationship between the rate of growth of z_b and the other terms exists which may require even smaller time steps than given by Equation (5.7) and proved to always be the controlling factor in determining an acceptable time step. For typical values of T/S of 10^8 - 10^9 m/day, the time step required by Equation (5.7) was in the order of 0.0001 days or less for typical values of Δx of 100-500 meters.

While such time steps may in fact be necessary for some problems requiring the complete model capabilities, these small time steps begin to increase computational time substantially, especially if one is interested in times on the order of months or years. Therefore, in trying to be consistent with one of the stated objectives of this project, to minimize computer time and storage requirements, alternative approaches were sought for use in appropriate cases. It is expected that drawdown will stabilize much more quickly than the other parameters. In fact, drawdown is expected to stabilize in about a day or so; in fact, for the Pinellas County situation in Chapter 6, the drawdown will stabilize within an hour. This rapid convergence of the drawdown, coupled with its severe constraint on allowable time step suggests two possible alternatives in the calculation procedure. First, one can proceed with the numerical scheme as is, but with provisions to begin bypassing Equations (5.1) and (5.3) when the drawdown reaches steady state (as measured by the rate of change falling below some specified level). A second approach would involve bypassing Equations (5.1) and (5.3) altogether and using an analytical method for calculation of the drawdowns. The particular method would depend on the aquifer situation in the area being modeled. Either one of these methods would relax the time step constraints, although the first method would still require small steps for a period of time. In the following paragraphs, the use of the second scheme will be outlined. Subsequent results will show that time steps of at least one day can be tolerated with the analytical scheme.

5.3 A Simplified Injection Model

By replacing Equation (4.32) with an analytical drawdown relationship, some simplifying assumptions must be made. It is assumed that the stratified conditions in the aquifer do not affect the drawdowns. This assumption was checked with field data from the United States Geological Survey report on injection wells in the Pinellas County, Florida area [Hickey, 1982] and was found to be valid.

5.3.1 Analytical Calculation of Head Build-up

There are many analytical methods available for the calculation of drawdowns due to the influence of a well. Theis [1935] developed a drawdown equation for unsteady flow in a confined aquifer.

$$\phi_o - \phi = \frac{Q}{4\pi T} \int_{y=u}^{\infty} \frac{e^{-y} dy}{y} \tag{5.9}$$

where Q = discharge or injectin rate of the well, T = transmissivity of the aquifer, and u is given by the following relationship:

$$u = \frac{r^2 S}{4Tt} \tag{5.10}$$

where r = radius from the well to the point evaluated, S = storativity of the aquifer, and t = time since the injection or pumping began.

The exponential integral in Equation (5.9) can be approximated by an infinite series

$$\int_u^{\infty} \frac{e^{-u} du}{u} = 0.5772 - \ln u + u - \frac{u^2}{2 \cdot 2!} + \frac{u^3}{3 \cdot 3!} - \cdots \tag{5.11}$$

for a small value of u, the sum of the series beyond u becomes negligible [Cooper and Jacob, 1946].

Although Equation (5.9) using (5.10), and (5.11) provides an accurate solution for a confined aquifer, it does not account for leakance in the confining layer. Since most practical applications would encounter leakance, it is desirable to account for leakance in the drawdown calculations.

Hantush and Jacob [1955] developed the following relationship describing the drawdown due to unsteady flow to a well in an infinite leaky confined aquifer.

$$\phi_o - \phi = \frac{Q}{4\pi T} \int_{y=u}^{\infty} \frac{1}{y} \exp\left(-y - \frac{(r/\lambda)^2}{4y}\right) dy \tag{5.12}$$

$$= \frac{Q}{4\pi T} W(u, r/\lambda) \tag{5.13}$$

where u is defined in Equation (5.10), r is the radius from the well, and

$$\lambda = \left(\frac{B'T}{K'}\right)^{1/2} \tag{5.14}$$

where λ is the leakage factor; T is the transmissivity of the aquifer; and K' is the thickness and permeability of the semi confining layers, respectively.

For a large r/λ value, the integral in Equation (5.12) can be approximated by a Taylor series expansion [Hunt, 1978]. A more simple and accurate representation is an asymptotic expansion by Wilson and Miller [1978].

$$W(u,\ r/\lambda) = \left(\frac{\Pi\lambda}{2r}\right)^{1/2} \exp\left(\frac{-r}{\lambda}\right) \operatorname{erfc}\left(-\frac{\frac{r}{\lambda} - zu}{2u^{1/2}}\right) \tag{5.15}$$

where erfc is the complementary error function.

The previous approximation was used extensively in this report. A problem occurs, however, in aquifers of high transmissivities, especially at locations close to the well where r/λ values are small and the assumption of large r/λ values is violated.

An alternate solution of equation (5.12) is to numerically integrate the integral using a numerical integration technique. This method yielded excellent results for calculation of drawdowns, and worked for a wide variety of injection situations.

In an effort to conserve computer resources, a relationship developed by Hantush was used to approximate equation (5.12). The assumption for the following relationship is that $u < r^2/20\lambda^2$ if $u < 1$ [Bear, 1979]

$$W(u,\ r/\lambda) = 2K_0(r/\lambda) - I_0(r/\lambda)\ W(Tt/S\lambda^2) \tag{5.16}$$

Where K_0 and I_0 are Bessel Functions that can be approximated using polynomial expansions. $W(Tt/S\lambda^2)$ is an exponential integral of a well function $W(u)$ where $u = Tt/S\lambda^2$.

An advantage of applying analytical drawdown calculations is that there are many types of equations that apply to many situations. In his book, Muskat [1937] describes an analytical means for accounting for partial penetration of the well in steady state drawdown calculations. Hantush also derived an infinite-series expansion equation that accounted for partial penetration in a leaky aquifer for unsteady flow [Bear 1979].

5.3.2 A Simplification of Equations (5.4) and (5.5)

If an analytical method is being used to calculate drawdowns, the finite difference approximation of head gradients can be eliminated or refined. Specific discharge is proportional to the head gradient. If the head gradient could be calculated analytically by differentiating the drawdown equation, an exact solution for the specific discharge could be obtained.

If differentiation of the drawdown equation is not practical, a more refined finite difference approximation can still be attained. Since drawdown can be calculated at any point, finite difference points for velocity calculation are not restricted to the points on the overall finite difference grid. To find head gradients at a point, drawdowns very close to that point at distances independent of the overall grid size, can be found and head gradients calculated using a finite difference scheme.

It was observed in the report by Means [1982] and in this report that drawdowns attain steady state conditions rapidly. For this reason it is reasonable to use in equation (4.47), drawdowns at the previous time step, thus making an explicit solution to Equation (4.47) possible.

By calculating the slopes, directly, and by using slopes at the previous time step, equation (4.47) is now approximated by

$$\left(\frac{n}{2}\int_0^1 L(n)dn\right)\frac{\delta_{i,j}^{2(m+1)}-\delta_{i,j}^{2(m)}}{\Delta t} - \left[\delta_{i,j}^{2(m)}\, k_{i,j}\left(\frac{\partial^2 s}{\partial x}+\frac{\partial^2 s}{\partial y}\right)\right.$$

$$\left. +\frac{1}{2}k_{i,j}\left(\frac{\partial s}{\partial x}\,\frac{\delta_{i,j}^{2(m)}-\delta_{i-1,j}^{2(m)}}{\Delta t}+\frac{\partial s}{\partial y}\,\frac{\delta_{i,j}^{2(m)}-\delta_{i,j-1}^{2(m)}}{\Delta x}\right)\right]\int_0^1 F(n)L(n)dn$$

$$= -a\left(\left(\frac{-\partial s}{\partial x}\right)^2+\left(\frac{-\partial s}{\partial y}\right)^2\right)^{1/2} L'(0) \tag{5.17}$$

Equation (5.17) can be solved for $\delta_{i,j}^{2(m+1)}$ explicitly.

5.3.3 General Solution Procedure

Since the modified version of the injection model calculates drawdowns analytically and calculates the transition zone thickness explicitly, only the equation for the thickness of the freshwater lens is solved iteratively. Figure 5.2 shows this procedure in a flow chart.

By reducing the number of equations to be iterated, and by solving equation (4.47) explicitly, computer resources are conserved greatly.

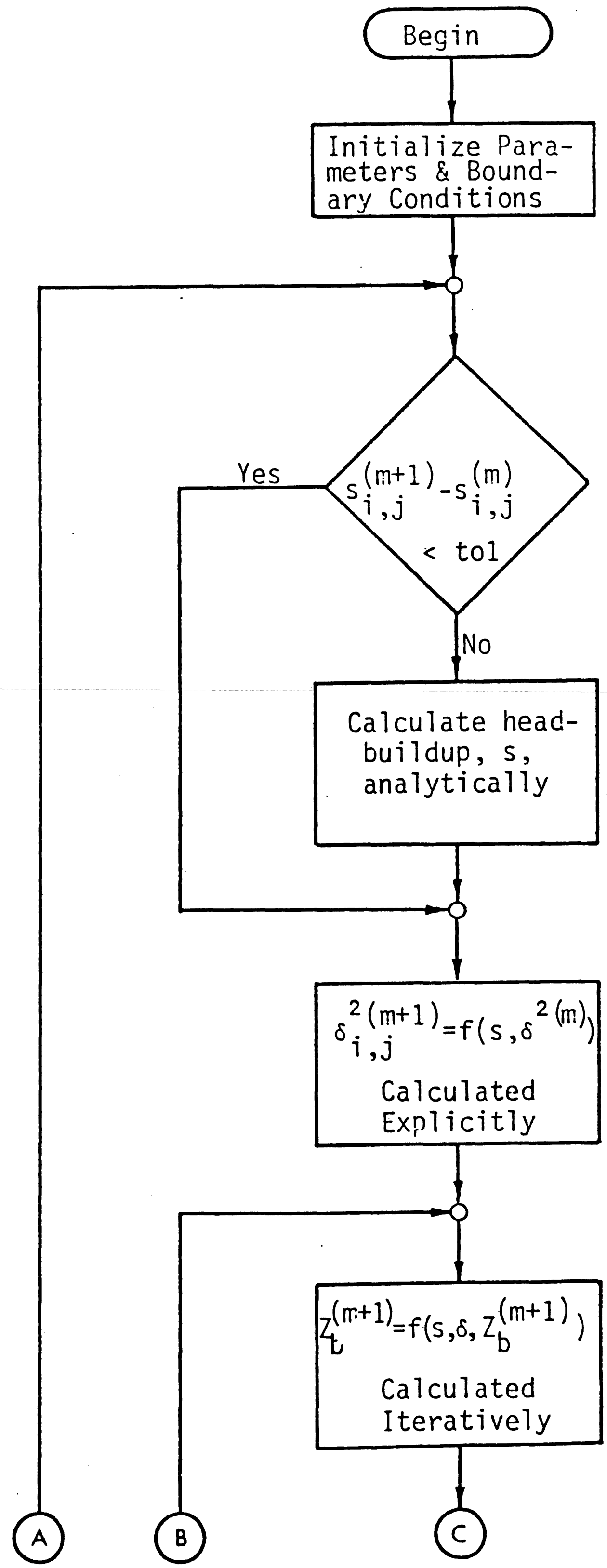

Figure 5.2 Flow Chart for modified model

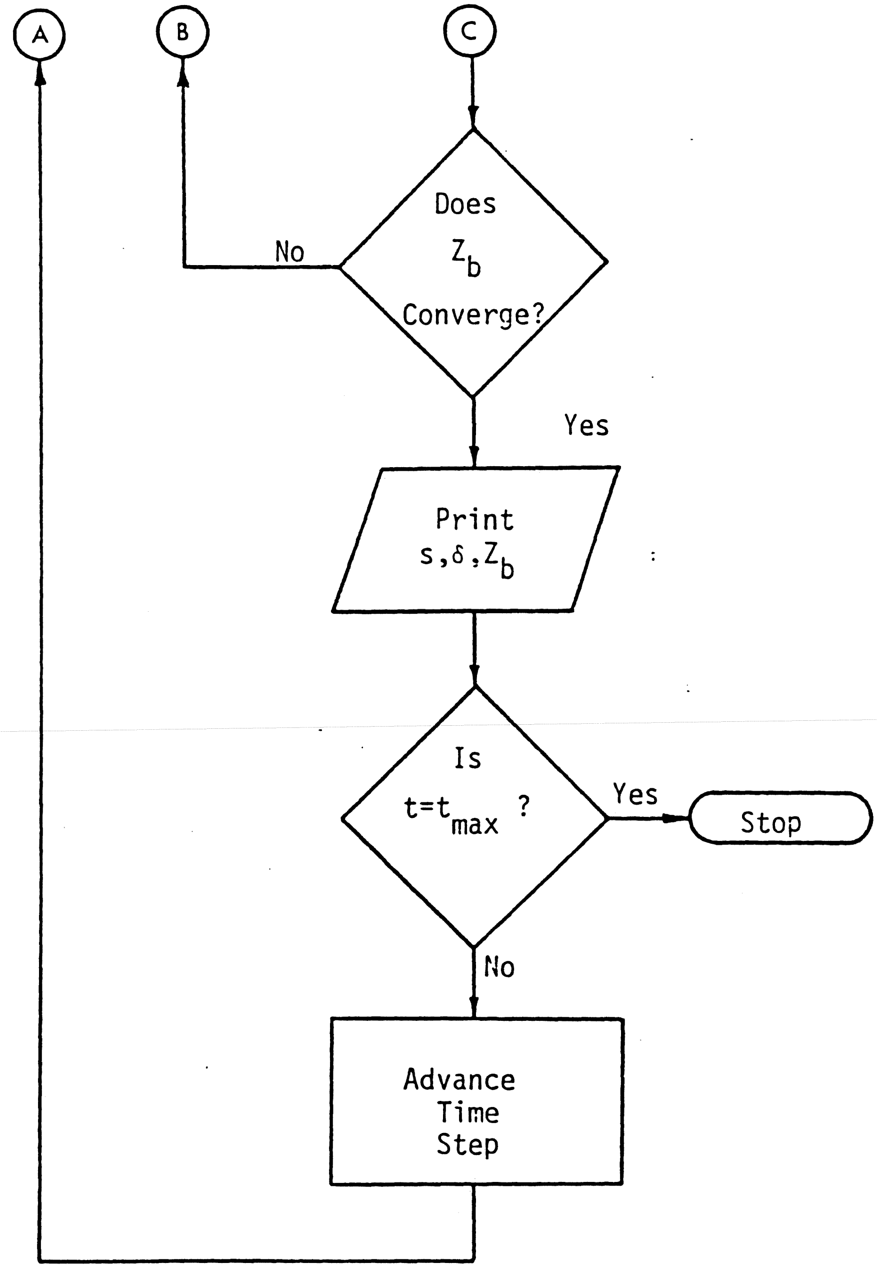

Figure 5.2 (Continued)

CHAPTER 6

VERIFICATION

6.1 Introduction

In this chapter final results from the previously developed injection model will be compared to a series of field injection-tests into a saline aquifer in Pinellas County, Florida. Field data is taken from a United States Geological Survey report entitled, "Hydrogeology and Results of Injection Tests at Waste-Injection Sites in Pinellas County, Florida" [Hickey 1982].

6.2 Geologic Framework of Pinellas County, Florida

Figure 6.1 Shows the geologic formations beneath St. Petersburg. The aquifer system underneath Pinellas County is mainly composed of several layers of sedimentary rocks ranging in age from Cretaceous to Pleistocene. The sedimentary rocks that make up the aquifers are mostly dolomite and limestone, which reach vertical thicknesses of approximately 10,000 to 12,000 feet. The stratigraphy of Pinellas county consists of several layers of sedimentary rocks, deposited over several geologic periods. The youngest deposits are the surficial sand deposits, which were deposited during the Pleistocene Epoch. Below the surficial deposit is the Hawthorn Formation, which was formed during the middle Miocene. Older formations in order of increasing age, are Tampa Limestone (Lower Miocene), Suwannee Limestone (Oligocene), Ocala Limestone (Upper Eocene), Avon Park Limestone (Middle Eocene), Lake City Limestone (Middle Eocene), and Oldsmar Limestone (Lower Eocene). Pinellas County is located on the southwest edge of the Peninsular Arch, which is the geologic backbone of the Florida peninsula, and is that

<table>
<tr><th>ERATHEM</th><th>SYSTEM</th><th colspan="2">SERIES</th><th>FORMATION</th></tr>
<tr><td rowspan="9">Cenozoic</td><td>Quaternary</td><td colspan="2">Pleistocene</td><td>Surficial sand</td></tr>
<tr><td rowspan="8">Tertiary</td><td rowspan="2">Miocene</td><td>Middle</td><td>Hawthorn Formation</td></tr>
<tr><td>Lower</td><td>Tampa Limestone</td></tr>
<tr><td colspan="2">Oligocene</td><td>Suwannee Limestone</td></tr>
<tr><td rowspan="4"></td><td>Upper</td><td>Ocala Limestone</td></tr>
<tr><td rowspan="2">Middle</td><td>Avon Park Limestone</td></tr>
<tr><td>Lake City Limestone</td></tr>
<tr><td>Lower</td><td>Oldsmar Limestone</td></tr>
<tr><td colspan="2">Paleocene</td><td>Cedar Keys Limestone</td></tr>
<tr><td>Mesozoic</td><td>Cretaceous</td><td colspan="3">Undifferentiated for this report</td></tr>
<tr><td>Pre-Mesozoic</td><td colspan="4">Undifferentiated for this report</td></tr>
</table>

Figure 6.1 Time-stratigraphic units and formations underlying Pinellas County and the city of St. Petersburg, Florida [From Applin and Applin (1944), Heath and Smith (1954), and Puri and Vernon (1964)]

area's most dominant subsurface feature. Pinellas County is also located southwest of the Ocala Uplift, which is a gentle, anticlinal flexure, and runs axially parallel to the Peninsular Arch. Previous studies [Puri and Vernon, 1964] reveal that there are extensive fracture patterns in the Ocala Uplift in the northern part of Pinellas County.

All of the strata beneath St. Petersburg are permeable to some degree; however some rock layers are much less permeable than others. For this reason certain layers are classified as aquifers and others as confining beds. Lohman et al. [1972] define an aquifer to be a formation, group of formations or part of a formation that contains sufficient permeable material to yield significant quantities of water to wells and springs. They define a confining bed to be a body of "impermeable material" stratgraphically adjacent to one or more aquifers. Confining beds are much less permeable than aquifers and restrict the flow between aquifers.

Figure 6.2 shows the aquifer system beneath St. Petersburg. In the U.S.G.S. study, two aquifers were identified, the surficial aquifer and the Floridan aquifer. Two confining beds were also identified. There is the upper confining bed of the Floridan aquifer, which separates the surficial aquifer from the Floridan aquifer. There is also the lower confining bed of the Floridan aquifer, which is mostly made up of Lake City Limestone.

The Floridan aquifer can be further divided into four permeable zones, each separated by three semi-confining beds, where semi-confining beds are less permeable than the permeable zones. In this study the four permeable zones have been labeled alphabetically where zone A is the shallowest within the aquifer and zone D is the deepest. Zone C is the permeable zone in which the injection tests will take place.

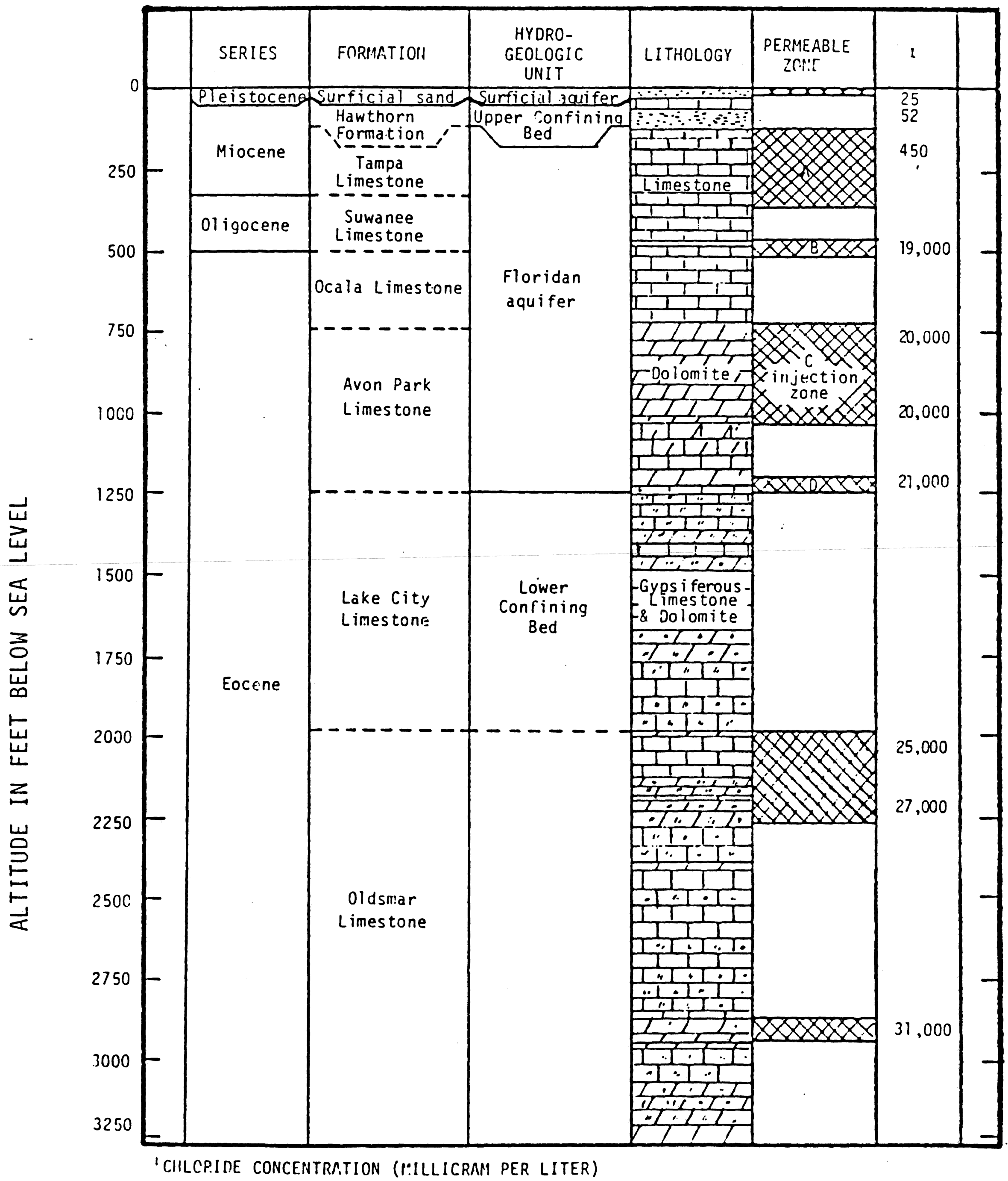

Figure 6.2 Aquifer system beneath St. Petersburg (from Hickey, 1982)

Most of the aquifer parameters were obtained using pumping tests, whereby observed drawdowns were matched with the corresponding pumping rates.

The water in the previously described aquifers is mostly saline, with a small layer of freshwater in the overlying surficial aquifer. Sources of the deeper saline water are the Gulf of Mexico and Tampa Bay, whereas the source of freshwater near the surface is rainwater that infiltrates from the surface. The salinity content ranges from 6 mg/L in the surficial aquifer to approximately 21,000 mg/L below the bottom permeable zone.

Small amounts of freshwater are tapped from the surficial aquifer for irrigation and municipal supplies; however, all water distributed by Pinellas County and the city of St. Petersburg is pumped from as far as 40 miles inland from Pinellas County.

6.3 Injection Tests

Injection tests were run at three locations: McKay Creek, South Cross Bayou, and southwest St. Petersburg. Well locations for the three tests are shown in Figure 6.3. Duration of tests ranged from 3 days at South Cross Bayou to 91.1 days at southwest St. Petersburg. Injection rates ranged from 650 gal/min at McKay Creek to 4,350 gal/min at South Cross Bayou.

6.3.1 Injection Tests at McKay Creek

The injection test at McKay Creek was run for 57.1 days; water with a chloride content ranging from 93 to 110 mg/L was injected at an average of 650 gal/min into permeable zone A. The well casings at the McKay Creek test site were open for the top sixty percent of the aquifer's thickness for well C1, and over forty percent of the aquifer's

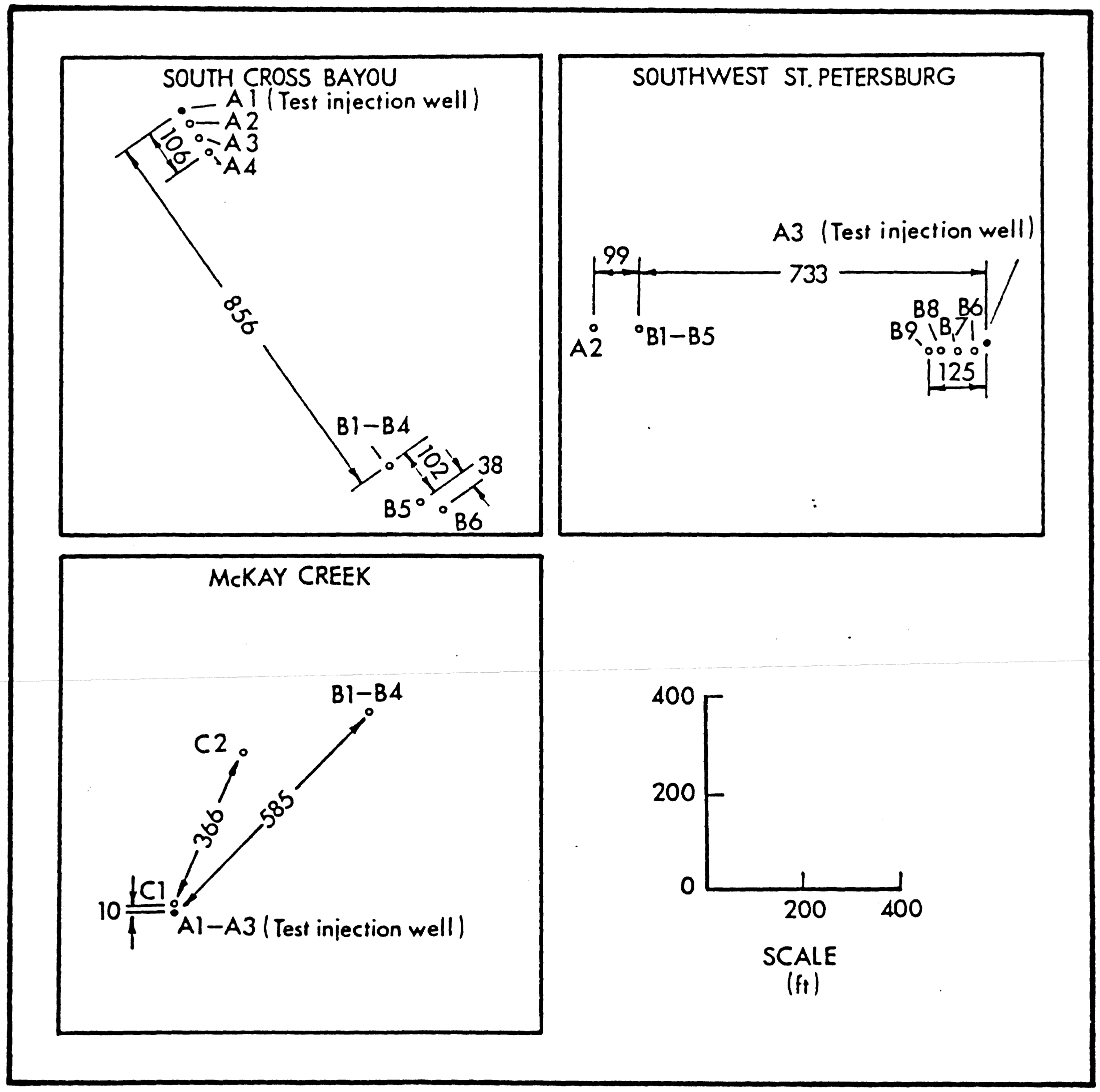

Figure 6.3 Locations of test wells in injection tests at South Cross Bayou, Southwest St. Petersburg and McKay Creek

thickness for well C2. Water quality and water level data were collected before, during and after the test. During the test, no substantial head increase was noticed; this is a result of the high tranmissivity of the injected aquifer. Chloride content in a well 585 feet from the injection well dropped from 20,000 mg/L before the test, to 18,000 mg/L after the test. A well directly above the injection interval experienced no change in chloride content, indicating inhomogeneity in the vertical permeability of zone A.

6.3.2 Injection Tests at South Cross Bayou

The South Cross Bayou injection test was run for three days by injecting water with an average chloride concentration of 710 mg/L at a rate of 4,350 gal/min into permeable zone C. The injection well's casing at South Cross Bayou was open over approximately the bottom 35% of the aquifer's thickness. The chloride concentration of the native water in the injection zone was 20,000 mg/L. Data such as pressure buildup and concentration changes caused by the injection are shown in Figure 6.4. It is noted that the pressure buildup at South Cross Bayou was very small, indicating a high transmissivity of the injected aquifer.

6.3.3 Injection Tests at Southwest St. Petersburg

The test at southwest St. Petersburg was run for 91.1 days. In this test, treated effluent from St. Petersburg's city wastewater treatment plant was injected into permeable zone C along with a tracer (rhodamine WT). The tracer was used to make detection of injected water in observation wells easier. The injection rate averaged 3,380 gal/min (standard deviation = 80 gal/min) for the first 9.1 days. For the remaining 82 days the injection rate was lowered to 2,770 gal/min

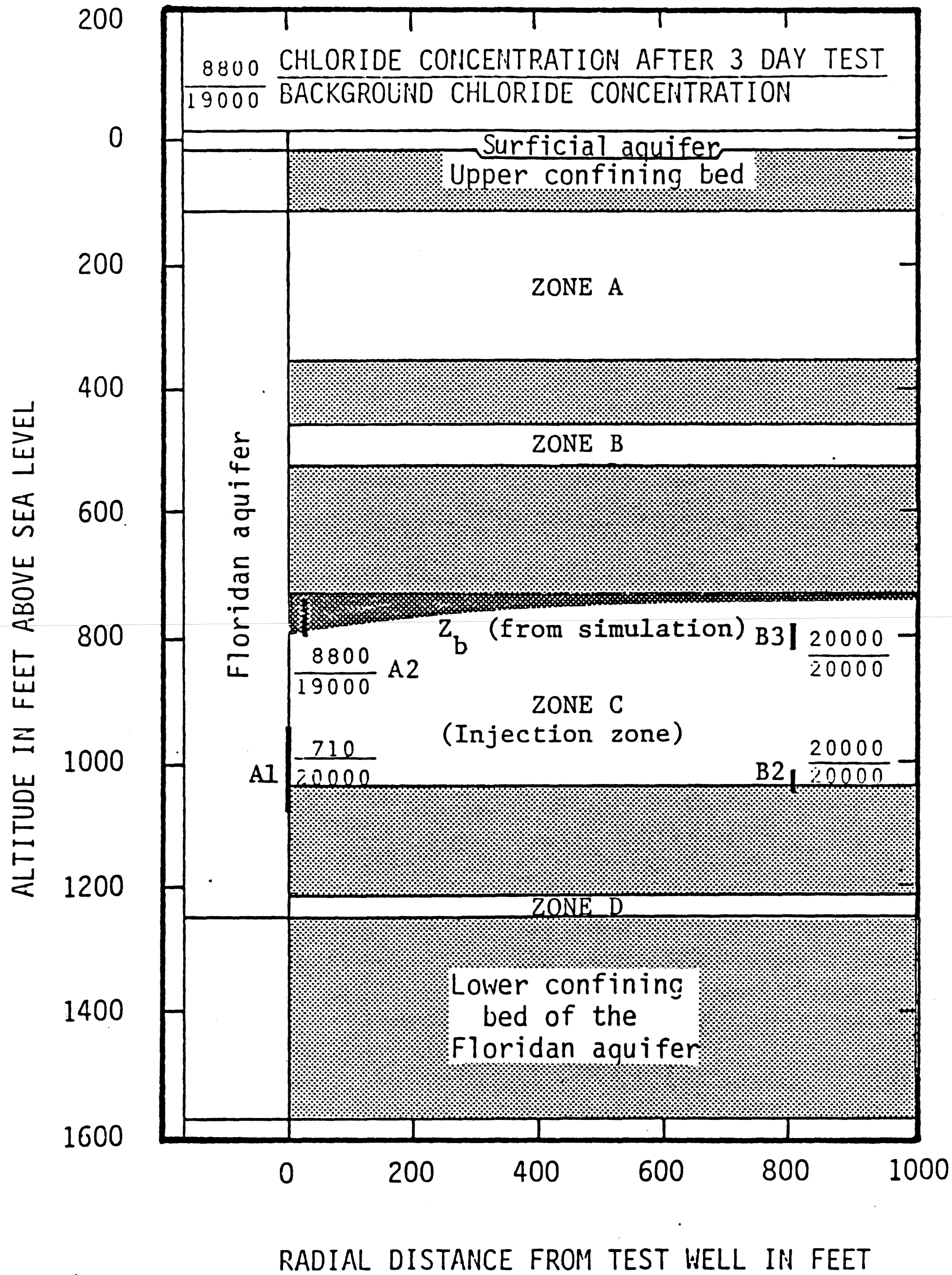

Figure 6.4 Comparison of field data to simulation results, South Cross Bayou

(standard deviation = 150 gal/min). The average injection rate for the entire test was 2,830 gal/min. The casing of the injection well in this test was open approximately over the lower sixty percent of the aquifer thickness.

Rhodamine WT was detected in a well directly above the injection point between 0.03 to 1.2 days from the start of the test. The tracer was also detected above the well in permeable zone B, indicating a "short circuit" in the vicinity of the injection well. The term "short circuit" is used since the tracer probably would not have leaked through the upper semi-confining layer had it not been disturbed. A well 733 feet from the injection well detected the tracer at the top of permeable zone C, but when used to sample the bottom portion of permeable zone C, no tracer was detected. This indicates that the injected water stratified due to density differences near the top of the injection zone. Data from the injection test can be seen in Figure 6.5.

6.4 Simulation of Injection Tests using the Simplified Injection Model

Using the simplified model described in section 5.3, computer simulations of the injection tests at South Cross Bayou and southwest St. Petersburg were made. The McKay Creek injection was not modeled as results from the test showed little impact. Input parameters used in the simulation are described in section 6.3 and in Table 6.1. Although a simulation was not run for the McKay Creek Injection test, parameters for the test are listed for completeness.

6.4.1 South Cross Bayou Simulation

The South Cross Bayou simulation was three days in duration; time steps for the numerical procedure were in increments of 0.1 day. The injection rate was 4,350 gal/min. The lowest leakance coefficient value

TABLE 6.1: Estimated aquifer coefficients for zone C (injection zone) based on aquifer test analyses

Test Site	Transmissivity T (ft^2/d)	Storage coefficient S	Storage coefficient from laboratory compressibility tests S	Leakance coefficient k'/b' (1/d)	Diffusivity T/S (ft^2/d)
S.W. St. Petersburg	1.2×10^{6}	3.3×10^{-4}	6.0×10^{-4}	2.2×10^{-4} to 1.9×10^{-3}	3.6×10^{9}
South Cross Bayou	1.2×10^{6}	2.2×10^{-4}	1.5×10^{-4}	3.7×10^{-4} to 1.5×10^{-3}	5.5×10^{9}
McKay Creek	0.9×10^{6}	0.8×10^{-4}	3.1×10^{-4}	6.6×10^{-3} to 1.5×10^{-2}	11.3×10^{9}

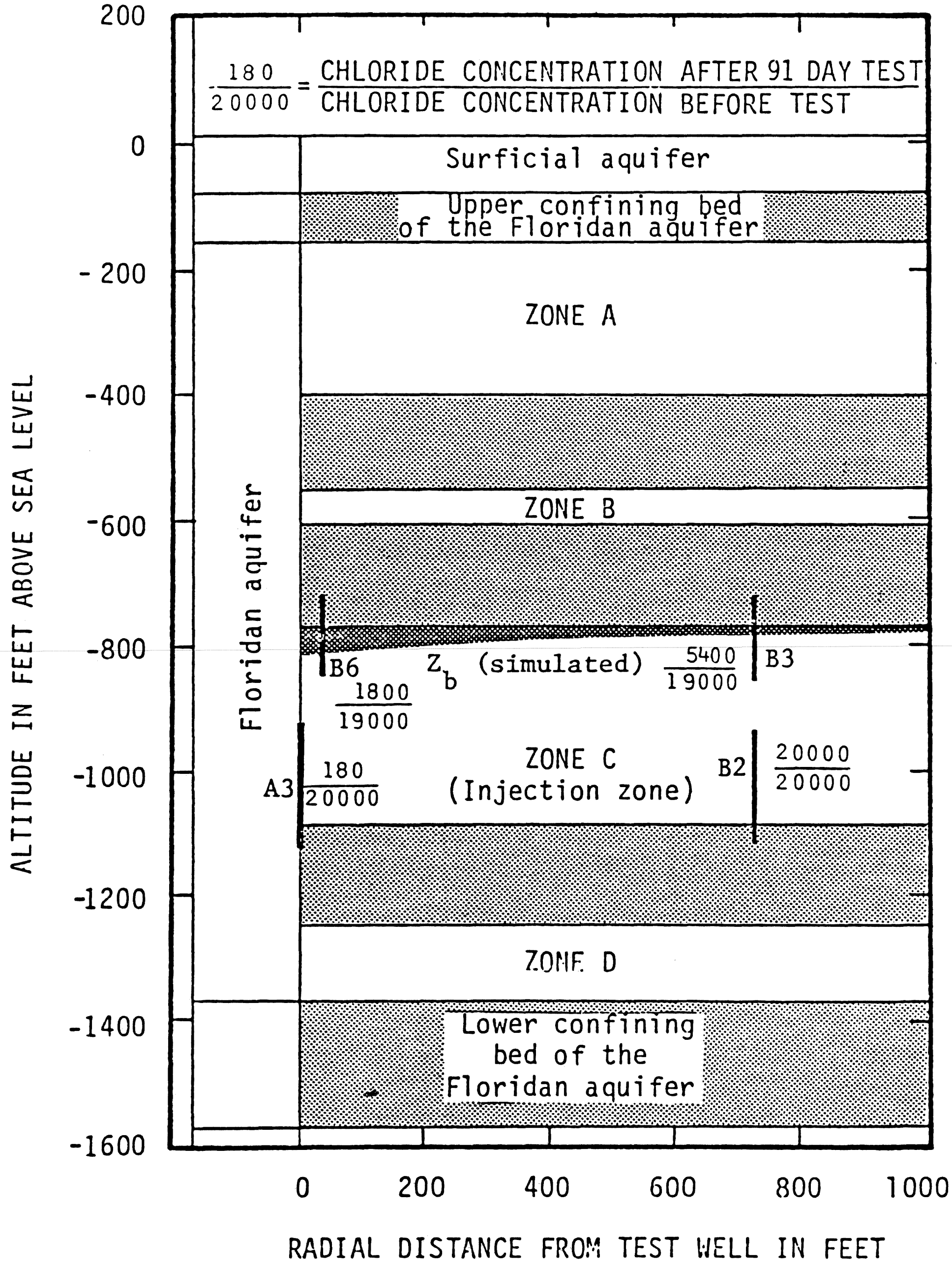

Figure 6.5 Comparison of field data to simulation results, Southwest St. Petersburg

was chosen from the range given in Table 6.1. Using the smallest leakance coefficient will result in a calculation of the maximum possible head build up which will provide the most conservative estimate of the effect of the injection well.

Results of the South Cross Bayou simulation are illustrated in Figure 6.4.

6.4.2 Southwest St. Petersburg Simulation

The simulation of the injection test at southwest St. Petersburg was 92 days in duration; time steps for the numerical procedure were in increments of 0.1 day for the first day and were increased to increments of 1 day after the first day of the simulation. Again the lowest leakance coefficient was chosen from the range given in Table 6.1 to provide the mose conservative results possible.

Results of the southwest St. Petersburg simulation are illustrated in Figure 6.5.

6.5 Comparison of Simulation to Injection Test Data

To compare the computer simulation to the field data, z_b (thickness of the freshwater lens) from the simulation is plotted on Figures 6.3 and 6.4 for South Cross Bayou and southwest St. Petersburg tests, respectively. Also listed in Figures 6.4 and 6.5 is the data from the injection tests at South Cross Bayou and southwest St. Petersburg, respectively.

Another method of comparison would be to integrate vertically over the transition zone to find concentration values that could be compared to the concentration values of the injection tests. This method would require an accurate estimation of the velocity and concentration of profiles within the transition zone. Since the exact velocity and concentration profiles are not known, measurements must be made before the concentration comparisons can be made. As noted earlier, exact values of the velocity and concentration profiles are not critical to the overall predictions. However, to calculate actual concentrations within the transition zones, a more accurate description must be used. This may be especially important in a situation such as here where salt water exists both above and below the injected water.

The results obtained from the simulation in both the South Cross Bayou and southwest St. Petersburg situations underestimate the influence of the injection well in the vicinity of the well. This discrepancy is probably due to the assumption of only horizontal flow in the freshwater region. By making the assumption of horizontal flow, the influence of vertical flow is neglected; in the vicinity of the well, vertical flow is likely to be of major influence. This is especially true due to the location of the injection wells at the bottom of the injection zone.

Some difficulties in convergence are encountered in the region of rapid head changes near and at the well.

It is possible that these difficulties can be eliminated if a more accurate description of the drawdown in the vicinity of the well is obtained. Work is continuing to refine the problems in the vicinity of the well.

Figures 6.4 and 6.5 indicate that the general extent of the injected water field is reasonably reproduced. While integrations of the concentration profile have not been attempted, Figure 6.4 (South Cross Bayou) indicates that the well nearest the injection well is partly in the injected water and partly in the saltwater. This seems consistent with the high chloride value observed there (8800 mg/l).

CHAPTER 7

CONCLUSIONS AND RECOMMENDATIONS

7.1 Conclusions

In this report, a three-dimensional model was developed in simulation of injection into a two-layered stratified aquifer. To account for effects in the flow field due to a transition zone of varying density and salt concentration between the fresh and saline layers an integral technique is used. By using an integral technique, the appropriate equations are simplified enough to be solved using an iterative ADI numerical scheme.

By taking advantage of the rapid stabilization of the head build-up, simplifications were made to the model which enhanced the stability characteristics and decreased the computer run time requirements of the model. Since the head build-up stabilizes quickly, it was possible to calculate the head build-up directly by using available analytical drawdown relationships. Because of the simplification of the head build-up calculation, the overall solution procedure was greatly simplified by eliminating the need for an overall iterative scheme. Also, because of the analytical calculation of the head build-up, flow velocities could be calculated directly, thus allowing for simplification of the calculation of the transition zone thickness.

To check accuracy of the model, simulations were made with the model using input data from injection tests in Pinellas County, Florida. Simulation output was compared to the actual results of the injection test. General features reproduced by the head build-up, transition zone thickness, and the thickness of the freshwater lens appear to be underestimated near the well.

Underestimation of the effect of the well is possibly a combination of several factors. First, since there are very high head gradients in the vicinity of the well, numerical problems become a factor. Also, the analytical head build up scheme presently used assumes radial flow, whereas the injection well is actually only partially penetrating the aquifer and curvature of the streamlines is present near the well. Also because of the curvature of the streamlines and buoyancy effects, the assumption of horizontal flow is not completely accurate in the vicinity of the well.

Work on the abovementioned problems is continuing and results will be available in a University of Florida Master of Engineering thesis by Laux in 1984.

7.2 Recommendations

The models presented in this report provides a basis for future refinements. It should provide the ability for users to make preliminary estimates of the behavior of injection fields in settings similar to that modeled herein. There are several areas where further work is needed, some of which is continuing now. The following topics seem most deserving of attention in terms of their potential for most improvement of the model.

1. Techniques should be developed to refine the numerical portion of the model solution in the vicinity of the well. This may lead to guidelines for selection of time and distance steps, as well as possibly modified finite-difference expressions.

2. The model should be modified to account for partial penetration of the well, both in terms of the expected head buildup and in terms of the flow field attained by the injected fluid.

3. Vertical flow effects should be incorporated into the model in at least two ways: the assessment of chlorides added to the injected water by the rising plume, and achieving a better description of the actual injection field.

4. The use of analytical calculations shows a head buildup occurring at some distance from the well at very short times. The model then responds to these head buildups by showing immediate arrival of injected water. However, there is quite likely a lag time associated with the actual arrival of the injected water. Neglect of this feature may lead to inaccuracies of the model when used for short duration events. Attempts should be made to investigate this factor.

5. The effect of the assumed profiles on predictions should be investigated by numerical experimentation with other profiles. This effort should also be extended to allow integration of the profiles to estimate chloride (or other constituent) concentrations at various wells.

6. The effect of the assumed flow directions should be investigated.

It is believed that the model which has been developed provides a useful tool for preliminary analysis of injection problems. It is expected that completion of some of the recommended items described will enhance its use.

APPENDIX

PROGRAM LISTING

```
C       A MODIFIED NUMERICAL-ANALYTICAL MODEL FOR THE SIMULATION
C       OF AN INJECTION INTO A CONFINED DENSITY-STRATIFIED AQUIFER.
C
C                            LIST OF ARRAYS
C
C              SN, SE, S= PRESENT, MEAN, PAST VALUES OF HEAD-BUILDUP
C              ZN, ZE, Z= PRESENT, MEAN, PAST VALUES OF FRESHWATER LENS
C              DZ= RATE OF CHANGE OF THICKNESS OF FRESHWATER LENS
C              DN2, D2=PRESENT, PAST SQUARED THICKNESS OF THE TRANSITION ZONE
C              DLN, DLE, DL= PRESENT, MEAN, PAST THICKNESS OF THE
C                          TRANSITION ZONE
        DIMENSION SE(50,50),S(50,50),ZN(50,50),ZE(50,50),Z(50,50)
        DIMENSION DZ(50,50),DN2(50,50),DLN(50,50),DLE(50,50),DL(50,50)
        DIMENSION D2(50,50)
        COMMON /NM/ N,M
        COMMON /DEL/ DX,DY,TIME
        COMMON /PARAM/ T,STO
        COMMON /DD/ SN(50,50)
        COMMON /NEW/ B1,B,XK
        COMMON /GOOD/ III(10),JJJ(10),QWELL(10),JI
        COMMON /MOI/ SXM(50,50),SXP(50,50),SYM(50,50),SYP(50,50)
        COMMON /HEY/ XD,YD
C       ***************************************************
C                    INPUT GRID DATA
C
C           N= NUMBER OF X-DIRECTION NODES     M= NUMBER OF Y-DIRECTION NODES
C           DX= DISTANCE BETWEEN X-DIR NODES  DY= DISTANCE BETWEEN Y-DIR NODES
C           DT= TIME INCREMENT
C           TIMAX= MAXIMUM TIME MODELED
C           XD= X-DISTANCE USED FOR FINITE-DIFFERENCE APPROXIMATION
C           YD= Y-DISTANCE USED FOR FINITE-DIFFERENCE APPROXIMATION
C       ***************************************************
        READ(5,200) N,M
        WRITE(6,400) N,M
        READ(5,205) DX,DY,DT,TIMAX
        WRITE(6,410) DX,DY,DT,TIMAX
        READ(5,207) XD,YD
        WRITE(6,412) XD,YD
C       ****************************************************
C                  INPUT AQUIFER DATA
C
C           T= TRANSMISSIVITY OF AQUIFER
C           STO= STORATIVITY OF AQUIFER
C           B1= THICKNESS OF AQUIFER
C           B= THICKNESS OF SEMI-CONFINING FORMATION
C           XK= VERTICAL CONDUCTIVITY OF SEMI-CONFINING FORMATION
C           PN= POROSITY OF AQUIFER
C           BET= INTEGRAL OF L(ETA)*D(ETA)
C           AL= L'(0)
C           A1= DISPERSIVITY
C           XKSI= DENSITY RATIO
C           AB= INTEGRAL OF F(ETA)*L(ETA)*D(ETA)
C       ****************************************************
        READ(5,210) T,STO
        WRITE(6,420) T,STO
        READ(5,220) B1,B,XK
        WRITE(6,430) B1,B,XK
        READ(5,250) PN,BET,AL,A1,XKSI,AB
        WRITE(6,440) PN,BET,AL,A1,XKSI,AB
C       ****************************************************
C                   INPUT WELL DATA
C
C           JI= NUMBER OF WELLS TO BE INPUT
C           III(IRD)= X-COORDINATE OF WELL IRD
C           JJJ(IRD)= Y-COORDINATE OF WELL IRD
C           QWELL(IRD)= INJECTION RATE OF WELL IRD
C       *****************************************************
        READ(5,230) JI
        WRITE(6,450) JI
        DO 2 IRD=1,JI
          READ(5,240) III(IRD),JJJ(IRD),QWELL(IRD)
          WRITE(6,460) III(IRD),JJJ(IRD),QWELL(IRD)
 2      CONTINUE
        PNL=PN*BET*0.5
        AL1=AL*A1
        XKK=T/(B1*PN*(1.0+XKSI))
        M1=M-1
        N1=N-1
C           INITIALIZE VECTORS AND ARRAYS
        DO 4 J=1,M
          DO 3 I=1,N
            SN(I,J)=0.0
            SE(I,J)=0.0
```

```
            S(I,J)=0.0
            DN2(I,J)=0.0
            D2(I,J)=0.0
            DLN(I,J)=0.0
            DLE(I,J)=0.0
            DL(I,J)=0.0
            DZ(I,J)=0.0
            ZN(I,J)=0.0
            ZE(I,J)=0.0
            Z(I,J)=0.0
 3        CONTINUE
 4      CONTINUE
        ICNT=0
        ISKIP=0
        TIME=0.0
C          INCREMENT TIME
 5      TIME=TIME+DT
        XKT=T*DT/(B1*DX**2)
        AK=T*DT*AB/B1
        ICNT=ICNT+1
        SBIG=0.0
        IF(ICNT.GE.3) ICNT=1
        IF(ISKIP.EQ.1) GO TO 25
C          CALCULATE HEAD-BUILDUP ANALYTICALY FOR PRESENT TIME-STEP
        CALL HANT
        DO 20 J=1,M
         DO 10 I=1,N
          SB=ABS(SN(I,J)-S(I,J))
          IF(SB .GT. SBIG) SBIG=SB
          SE(I,J)=(SN(I,J) + S(I,J))/2.0
          S(I,J)=SN(I,J)
 10     CONTINUE
 20     CONTINUE
        IF(SBIG.LT.0.01) ISKIP=1
C          IF HEAD-BUILDUP REACHES STEADY-STATE, DO NOT RECALCULATE
C          HEAD-BUILDUP
        IF(ISKIP .EQ. 1)WRITE(6,22)
 22     FORMAT(1X,' ********************'/'  STEADY STATE REACHED'/
      $'  ********************')
 25     DO 40 J=2,M1
         DO 30 I=2,N1
         JJ=J
         II=I
        SCK=(SN(I,J)-SN(I-1,J))/DX
        SCK2=(SN(I,J)-SN(I,J-1))/DY
C          CALCULATE VELOCITIES (HEAD-GRADIENTS) USING VARIABLE-
C          SPACING FINITE DIFFERENCE APPROXIMATION
        DSDX=(SN(I,J)-SXM(I,J))/XD
        DSDY=(SN(I,J)-SYM(I,J))/YD
        D2DX=(SXP(I,J)-2.0*SN(I,J)+SXM(I,J))/XD**2
        D2DY=(SYP(I,J)-2.0*SN(I,J)+SYM(I,J))/YD**2
C          CHECK SLOPE OF HEAD-GRADIENT FOR SYMMETRY CONTROL
        IF(SCK.LT.0) DSDX=(SXP(I,J)-SN(I,J))/XD
        IF(SCK.LT.0) II=I+1
        IF(SCK2.LT.0) DSDY=(SYP(I,J)-SN(I,J))/YD
        IF(SCK2.LT.0) JJ=J+1
C          CALCULATE THE SQUARED THICKNESS OF THE TRANSITION ZONE
        DN2(I,J)=(D2(I,J)*PNL+AK*(D2(I,J)*(D2DX+D2DY)
      $ +0.5*DSDX*(D2(II,J)-D2(II-1,J))/DX
      $ +0.5*DSDY*(D2(I,JJ)-D2(I,JJ-1))/DY)
      $ -AL1*AK/AB*SQRT(DSDX**2+DSDY**2))/PNL
        IF(TIME.LT.7.1.OR.TIME.GT.20.) GO TO 30
        IF(J.LT.9.OR.J.GT.11) GO TO 30
        IF(I.LT.9.OR.I.GT.11) GO TO 30
        WRITE(6,4321) I,J,II,JJ,D2(I,J),D2(II,J),D2(II-1,J),
      $ D2(I,JJ),D2(I,JJ-1),DSDX,DSDY,D2DX,D2DY,DN2(I,J)
 4321   FORMAT(1X,' I=',I3,' J=',I3,' II=',I3,' JJ=',I3,' D2(I,J)=',
      $ F8.3,' D2(II,J)=',F8.3,' D2(II-1,J)=',F8.3,' D2(I,JJ)=',
      $ F8.3,' D2(I,JJ-1)=',F8.3/' DSDX=',F10.5,' DSDY=',F10.5,
      $ ' D2DX=',F10.5,' D2DY=',F10.5,' DN2(I,J)=',F8.3)
 30       CONTINUE
 40     CONTINUE
        DO 100 J=2,M1
         DO 90 I=2,N1
          IF(DN2(I,J).LT.0) DN2(I,J)=0.0
          DLN(I,J)=SQRT(DN2(I,J))
          IF(DLN(I,J).GE.Z(I,J)) DLN(I,J)=Z(I,J)
          DLE(I,J)=(DLN(I,J) + DL(I,J))/2.0
          DL(I,J)=DLN(I,J)
          D2(I,J)=DN2(I,J)
          ZBZ=ZN(I,J)
C          ITERATIVELY CALCULATE THE THICKNESS OF THE FRESHWATER LENS
          DO 85 JIT=1,20
           DZ(I,J)=XKK/(B1-ZE(I,J))*(SN(I,J)+XKSI*(-ZE(I,J)
```

```
      $      +BET*XKSI*DLE(I,J)))
             ZN(I,J)=Z(I,J)+DZ(I,J)*DT
             ZB=ABS(ZN(I,J) - ZBZ)
             ZE(I,J)=(ZN(I,J) + Z(I,J))/2.0
C            WRITE(6,555) DZ(I,J),ZN(I,J),Z(I,J),ZBZ,ZB,ZE(I,J),I,J,JIT
C     $ ,DLE(I,J),DLN(I,J),DL(I,J),BET,XKSI,XKK,XKT
C555   FORMAT(1X,' DZ=',F7.2,' ZN=',F7.2,' Z=',F7.2,' ZBZ=',F7.2,
C     $ ' ZB=',F7.2,' ZE=',F7.2,' I=',I2,' J=',I2,' JIT=',I2
C     $ /' DLE=',F10.2,' DLN=',F10.2,' DL=',F10.2,' BET=',F6.4,
C     $ ' XKSI=',F6.4,' XKK=',F10.1,' XKT=',F12.2)
             IF(ZB .LT. 0.01) GO TO 87
             ZBZ=ZN(I,J)
 85        CONTINUE
           WRITE(6,86) I,J
 86      FORMAT(1X,' DZ DID NOT CONVERGE (20 IT) AT I=',I3,' J=',I3)
 87        Z(I,J)=ZN(I,J)
 90       CONTINUE
 100     CONTINUE
C        IF(TIME.GE.1.0) DT=1.0
C        IF(TIME.LT.0.184) GO TO 5
         IF(ICNT.EQ.1) GO TO 5
C           PRINT CYCLE
         WRITE(6,299) TIME
         DO 106 J=1,M
           WRITE(6,300) (S(I,J), I=1,N)
 106     CONTINUE
         WRITE(6,310)
         DO 107 J=1,M
           WRITE(6,320) (DL(I,J), I=1,N)
 107     CONTINUE
         WRITE(6,330)
         DO 108 J=1,M
           WRITE(6,340) (Z(I,J), I=1,N)
 108     CONTINUE
         IF(TIME.LT.TIMAX) GO TO 5
         STOP
 200     FORMAT(2I2)
 205     FORMAT(2F6.1,F7.3,F6.1)
 207     FORMAT(2F7.3)
 210     FORMAT(F10.2,F7.5)
 220     FORMAT(2F6.1,F8.4)
 230     FORMAT(I3)
 240     FORMAT(2I2,F10.1)
 250     FORMAT(F4.2,F6.4,2F6.3,F5.3,F8.4)
 299     FORMAT(1X//' HEAD BUILDUP AT TIME=',F10.3//)
 300     FORMAT(1X,50F6.3)
 310     FORMAT(1X//' THICKNESS OF TRANSITION ZONE'//)
 320     FORMAT(1X,50F6.3)
 330     FORMAT(1X//' PENETRATION OF FRESHWATER LENS'//)
 340     FORMAT(1X,50F6.3)
 400     FORMAT(1X,' N=',I2,' M=',I2)
 410     FORMAT(1X,' DX=',F6.1,' DY=',F6.1,' DT=',F6.2,' TIMAX=',F6.2)
 412     FORMAT(1X,' XD=',F8.4,' YD=',F8.4)
 420     FORMAT(1X,' T=',F10.1,' S=',F10.6)
 430     FORMAT(1X,' B1=',F10.1,' B=',F10.1,' XK=',F10.4)
 440     FORMAT(1X,' PN=',F6.4,' BET=',F6.4,' AL=',F6.3,' A1=',F7.4/
      $      ' XKSI=',F6.3,' AB=',F8.4)
 450     FORMAT(1X,' J1=',I4)
 460     FORMAT(1X,' III=',I4,' JJJ=',I4,' QWELL=',F10.1)
         END
         SUBROUTINE HANT
C           SUBROUTINE CALCULATES HEAD-BUILDUP IN AQUIFER USING
C           ANALYTICAL RELATIONSHIPS
         COMMON /DD/ DOWN(50,50)
         COMMON /NM/ N,M
         COMMON /DEL/ DELX,DELY,TIME
         COMMON /PARAM/ T,STO
C        WRITE(6,200) STO
C200     FORMAT(1X,' STO=',F10.5)
         CALL BEGIN
         CALL CONST
         CALL BDAY
C        WRITE(6,100) T,STO
C        WRITE(6,110) DELX,DELY
         RETURN
C100     FORMAT(1X,' TRANSMISSIVITY=',F10.1/'  STORATIVITY=',F10.4)
C110     FORMAT(1X,' DELX=',F10.2/'  DELY=',F10.2)
         END
         SUBROUTINE BEGIN
C           SUBROUTINE SETS UP REQUIRED SPATIAL VECTORS
         COMMON /NM/ N,M
         COMMON /DEL/ DELX,DELY,TIME
         COMMON /XY/ X(50),Y(50)
         COMMON /PARAM/ T,STO
```

```
      DO 5 I=1,N
          X(I)=(I-1)*DELX
 5    CONTINUE
      DO 7 J=1,M
          Y(J)=(J-1)*DELY
 7    CONTINUE
      RETURN
      END
        SUBROUTINE CONST
C       COMPUTE CONSTANTS
C
        IMPLICIT COMPLEX (C)
C
        COMMON  /MATH/            PI, EPS
        COMMON  /OMEGA/          COMREF, CC
C
        C=(0.,1.)
        CC=(0.,0.)
        PI=4.0*ATAN(1.0)
        EPS=1.0
  1     EPS=EPS/2.0
        EPSO=EPS+1.0
        IF (EPSO.GT.1.0) GOTO 1
        RETURN
        END
      SUBROUTINE BDAY
      COMMON /PUSH/ RB
      COMMON /NEW/ B1,B,XK
      COMMON /GOOD/ III(10),JJJ(10),QWELL(10),JI
      COMMON /NM/ N,M
      COMMON /DEL/ DELX,DELY,TIME
      COMMON /XY/  X(50), Y(50)
      COMMON /PARAM/  T,STO
      COMMON /MATH/ PI,EPS
      COMMON /DD/  DOWN(50,50)
      COMMON /MOI/ SXM(50,50),SXP(50,50),SYM(50,50),SYP(50,50)
      COMMON /HEY/ XD,YD
      DO 5 J=1,M
          DO 3 I=1,N
              DOWN(I,J)=0.00
              SXP(I,J)=0.00
              SXM(I,J)=0.00
              SYP(I,J)=0.00
              SYM(I,J)=0.00
 3        CONTINUE
 5    CONTINUE
      XK1=T/B1
      K=0
C        INCREMENT INJECTION WELL
 10   K=K+1
      II=III(K)
      JJ=JJJ(K)
      QW=QWELL(K)
      XW=X(II)
      YW=Y(JJ)
C        CALCULATE VALUES FOR EACH POINT ON SPATIAL GRID
      DO 30 J=1,M
          DO 20 I=1,N
C             CALCULATE RADIUS AT AND AROUND DESIRED GRID-POINT
             R=SQRT((X(I)-XW)**2+(Y(J)-YW)**2)
             RXP=SQRT((X(I)+XD-XW)**2+(Y(J)-YW)**2)
             RXM=SQRT((X(I)-XD-XW)**2+(Y(J)-YW)**2)
             RYP=SQRT((X(I)-XW)**2+(Y(J)+YD-YW)**2)
             RYM=SQRT((X(I)-XW)**2+(Y(J)-YD-YW)**2)
             IF (R.NE.0) GO TO 14
             R=0.10
             RXP= XD-0.1
             RXM= XD-0.1
             RYP=YD-0.1
             RYM=YD-0.1
 14          AMULT=SQRT(XK/(XK1*B1*B))
C             CALCULATE LEAKANCE PARAMATER AT AND AROUND GRID-POINT
C             (FIRST WELL FUNCTION PARAMETER)
             RB=R*AMULT
             RBXP=RXP*AMULT
             RBXM=RXM*AMULT
             RBYP=RYP*AMULT
             RBYM=RYM*AMULT
             BMULT=STO/(4.0*T*TIME)
C             CALCULATE SECOND WELL FUNCTION PARAMETER
             U=R**2*BMULT
             UXP=RXP**2*BMULT
             UXM=RXM**2*BMULT
             UYP=RYP**2*BMULT
```

```
                 UYM=RYM**2*BMULT
C                  CALCULATE WELL FUNCTION AT AND AROUND A GRID POINT
                 CE=XCOEF(U)
                 RB=RBXP
                 CXP=XCOEF(UXP)
                 RB=RBXM
                 CXM=XCOEF(UXM)
                 RB=RBYP
                 CYP=XCOEF(UYP)
                 RB=RBYM
                 CYM=XCOEF(UYM)
                 CMULT=QW/(4.0*PI*T)
C                  CALCULATE HEAD-BUILDUP AT AND AROUND GRID-POINT
                 DOWN(I,J)=CE*CMULT+DOWN(I,J)
                 SXP(I,J)=CXP*CMULT+SXP(I,J)
                 SXM(I,J)=CXM*CMULT+SXM(I,J)
                 SYP(I,J)=CYP*CMULT+SYP(I,J)
                 SYM(I,J)=CYM*CMULT+SYM(I,J)
C          WRITE(6,5432) I,J,R,RB,U,CE,DOWN(I,J)
C5432      FORMAT(1X,' I=',I3,' J=',I3,' R=',F10.3,' RB=',E10.3,' U=',
C     $     E10.3,' CE=',E10.3,' DOWN=',F10.3)
 20            CONTINUE
 30            CONTINUE
C         WRITE(6,150) TIME
C         DO 70 J=1,M
C              WRITE(6,140) (DOWN(I,J), I=1,N)
C70       CONTINUE
          IF(K.LT.JI) GO TO 10
          RETURN
C150      FORMAT(1X,'DRAWDOWN AT TIME=',F10.2)
C140      FORMAT(1X,50F6.2)
          END
          DOUBLE PRECISION FUNCTION XCOEF(U)
C             SUBROUTINE CALCULATES WELL FUNCTION FOR INPUT PARAMETERS
C
C                 WELL FUNCTION FOR A LEAKY AQUIFER--USING NUMERICAL
C                 INTEGRATION OF THE WELL FUNCTION
C
C                                   INPUT GUIDE
C
C                    INPUT IS PASSED TO SUBROUTINE IN THE CALL STATEMENT
C                    AND IN A COMMON STATEMENT
C
C                    RB= PARAMETER # 2.... PASSED THROUGH COMMON
C
C             WILL CALCULATE THE WELL FUNCTION FOR SPECIFIC PARAMETERS
C
C
C             THIS SUBROUTINE CAN BE SUBSTITUTED BY ANY SUBROUTINE THAT
C             CALCULATES THE WELL FUNCTION GIVEN THE NECESSARY INPUT
C             PARAMETERS.
              REAL*8 U,RB,XCOEF,ANS
          EXTERNAL FFX
          COMMON /PUSH/ RB
          AA=20.0
          EPSS=0.05
          MAXIT=25
C             CALL SCHEME TO NUMERICALLY INTEGRATE THE WELL FUNCTION
          CALL QA04AD(ANS,U,AA,EPSS,MAXIT,FFX)
          XCOEF=ANS
          RETURN
          END
          DOUBLE PRECISION FUNCTION FFX(X)
C             SUBROUTINE SUPPLYS THE WELL FUNCTION TO SUBROUTINE QA04AD
          REAL*8 RB,X,A,FFX
          COMMON /PUSH/ RB
          A=RB**2/(4.0*X)
          A=X+A
          FFX=DEXP(-A)/X
          RETURN
          END
C    QA04AD - A SUBROUTINE TO APPROXIMATE
C
C                                                  AA
C                                                 I   F(X)DX,
C                                                  BB
C
C    USING AN ADAPTIVE 3-POINT GAUSSIAN INTEGRATION SCHEME.
C
          SUBROUTINE QA04AD(ANS,AA,BB,EPSS,MAXIT,F)
          IMPLICIT REAL*8 (A-H,O-Z)
          REAL*8 R(30),B(30),B1(30),A1(30),EPS(30),EST2(30),EST3(30),FW(30),
         1FV(30),F3(30),F4(30),F5(30),F6(30)
          REAL*8 F
```

```
      DIMENSION J(30)
      COMMON/QA04BD/DIVD,LPD,NFD,ERREST
      COMMON /QA04B/DIVS,LPS,NFS,ESTS
      REAL*4 DIVS,ESTS,SANS,SAA,SBB,SEPS
C
C   THE ARGUEMENT LIST IS AS FOLLOWS:-
C   ANS     ON ENTRY:UNDEFINED.ON RETURN:SET BY THE SUBROUTINE TO THE
C           APPROXIMATION OF THE INTEGRAL I.
C   AA      ON ENTRY:SET BY THE USER TO THE UPPER LIMIT OF THE INTEGRAL.
C           ON RETURN:NO CHANGE.
C   BB      ON ENTRY:SET BY THE USER TO THE LOWER LIMIT OF THE INTEGRAL I.
C           ON RETURN:NO CHANGE.
C   EPSS    ON ENTRY:SET BY THE USER TO THE RELATIVE ACCURACY REQUIRED.
C           ON RETURN:NO CHANGE.
C
C   MAXIT ON ENTRY:IS THE MAXIMUM NO. OF ITERATIONS TO BE ALLOWED.
C           (LE.30) ON RETURN:CONTAINS THE MAXIMUM NO. OF ITERATIONS
C           ACHIEVED.
C   F         IS THE FUNCTION F(X) TO BE INTEGRATED.MUST BE SET BY THE
C           USER.
C
C
C           P AND Q ARE ONE HALF OF THE THREE POINT GAUSS-LEGENDRE WEIGHTS.
      DATA P,Q /4.444444444444444D-01,2.777777777777778D-01/
C
C           R(K)=R**K,WHERE R=1-SQRT(15)/5 USED FOR GENERATION OF POINTS OF
C           SUBDIVISION.
      DATA R(1)/2.254033307585167D-01/,R(2)/5.080666151703326D-02/,
     1R(3)/1.145199073065985D-02/,R(4)/2.581316854506389D-03/,
     2R(5)/5.818374167488376D-04/,R(6)/1.311480916951191D-04/,
     3R(7)/2.956121669070321D-05/,R(8)/6.663196703358761D-06/,
     4R(9)/1.501906730436233D-06/,R(10)/3.385347795289606D-07/,
     5R(11)/7.630686688342781D-08/,R(12)/1.719982195527138D-08/,
     6R(13)/3.876897157171633D-09/,R(14)/8.738655322347104D-10/,
     7R(15)/1.969722016007677D-10/,R(16)/4.439819030765107D-11/,
     8R(17)/1.000749997499504D-11/,R(18)/2.255723826929655D-12/,
     9R(19)/5.084476638612921D-13/,R(20)/1.146057969507219D-13/,
     1R(21)/2.583252835692698D-14/,R(22)/5.822737933565171D-15/,
     2R(23)/1.312464524359553D-15/,R(24)/2.958338752930355D-16/,
     3R(25)/6.668194084224985D-17/,R(26)/1.503033156728549D-17/,
     4R(27)/3.387886797671025D-18/,R(28)/7.636409684278539D-19/,
     5R(29)/1.721272177872976D-19/,R(30)/3.879804820345346D-20/
C
C           S=(1-R)/R.USED FOR GENERATION OF POINTS OF SUBDIVISION.
      DATA S/3.436491673103706D00/
C
C           DIV IS ADAPTIVE DIVISOR OF EPS(I)
      DIV=DIVD
      LP=LPD
   90 IERRC=0
      ERREST=0.D0
      IF(MAXIT.GT.30)MAXIT=30
      II=1
      ANS=0D0
      J(1)=4
      A=AA
      B(1)=BB
      BT=BB
      R1=BB-AA
      R2=0.1127016653792583D0*R1
C           R2=(1-SQRT(3/5))/2*R1
      FU=P*F(AA+R2)
      FV(1)=P*F(5D-1*(AA+BB))
      FW(1)=P*F(BB-R2)
      NF=3
      EST=R1*(625D-3*(FU+FW(1))+FV(1))
      ABSA=DABS(EST)
      EPS(1)=EPSS
      IMAX=1
      K=1
   10 I=II
      IF(I.GT.IMAX)IMAX=I
C           FORM GAUSSIAN SUMS AND TEST.
      R1=R(K)*(BT-A)
      A1(I)=A+R1
      B1(I)=A+S*R1
      R2=2D-1*(B(I)-A)
      W1=A+R2
      U3=B(I)-R2
      F1=F(A1(I)-R2)
      F2=F(W1)
      F3(I)=F(2D0*W1-5D-1*(A+A1(I)))
      F4(I)=F(2D0*U3-5D-1*(B(I)+B1(I)))
      F5(I)=F(U3)
      F6(I)=F(B1(I)+R2)
```

```
      NF=NF+6
      EST1=R1*(Q*(F1+F2)+FU)
      EST2(I)=(B1(I)-A1(I))*(Q*(F3(I)+F4(I))+FV(I))
      EST3(I)=R1*(Q*(F5(I)+F6(I))+FW(I))
      SUM=EST1+EST2(I)+EST3(I)
      ABSA=ABSA+DABS(EST1)+DABS(EST2(I))+DABS(EST3(I))-DABS(EST)
      IF(DABS(SUM-EST).LE.EPS(I)*ABSA)GO TO 20
C        IF NO. OF ITERATIONS ACHIEVED IS GREATER THAN NO. REQUESTED,
C       PRINT DIAGNOSTIC AND RETURN.
      IF(I.GE.MAXIT)GO TO 70
C       DEFINE LEFTMOST SUBINTERVAL.
      K=K+1
      II=I+1
      B(II)=A1(I)
      FW(II)=P*F2
      FV(II)=FU
      FU=P*F1
      EST=EST1
      EPS(II)=EPS(I)/DIV
      J(II)=1
      GO TO 10
C       WHEN ACCURACY IS REACHED AT ONE LEVEL,PROCEED TO NEXT
C       APPROPRIATE LEVEL.
   20 JJ=J(I)
      ERREST=ERREST+DABS(SUM-EST)
      I=I-1
      GO TO (30,40,50,60),JJ
C       DEFINE MIDDLE SUBINTERVAL.
   30 ANS=ANS+SUM
      K=1
      II=I+1
      A=A1(I)
      B(II)=B1(I)
      BT=B(II)
      FU=P*F3(I)
        FV(II)=FV(I)
      FW(II)=P*F4(I)
      EST=EST2(I)
      EPS(II)=EPS(I)/DIV
      J(II)=2
      GO TO 10
C       DEFINE RIGHTMOST SUBINTERVAL.
   40 ANS=ANS+SUM
      II=I+1
      A=B1(I)
      B(II)=B(I)
      BT=B(II)
      FU=P*F5(I)
      FV(II)=FW(I)
      FW(II)=P*F6(I)
      EST=EST3(I)
      EPS(II)=EPS(I)/DIV
      J(II)=3
      GO TO 10
   50 ANS=ANS+SUM
      SUM=0D0
      EST=0D0
      GO TO 20
   60 MAXIT=IMAX
      IF(NF.EQ.9)ANS=SUM
      IF(IERRC.LE.0)GO TO 100
      WRITE(LP,81)IERRC
   81 FORMAT(' QA04A/AD ACCURACY SUSPECT AT',I6,' POINTS',
     1' IN RANGE.       BEST ESTIMATE RETURNED.')
      MAXIT=-MAXIT
  100 SANS=ANS
      NFS=NF
      NFD=NF
      ERREST=ERREST*.01536D0
      ESTS=ERREST
      RETURN
C       REQUIRED ACCURACY NOT REACHED IN MAXIT ITERATIONS.
   70 IERRC=IERRC+1
      GO TO 20
      ENTRY QA04A(SANS,SAA,SBB,SEPS,MAXIT,F)
      DIV=DIVS
      LP=LPS
      AA=SAA
      BB=SBB
      EPSS=SEPS
      GO TO 90
      END
      BLOCK DATA
      REAL*8 DIVD,ERREST
```

```
COMMON/QA04BD/DIVD,LPD,NFD,ERREST
COMMON /QA04B/DIVS,LPS,NFS,ESTS
REAL*4 DIVS,ESTS
DATA DIVD/1.4D0/,LPD/6/,DIVS/1.4/,LPS/6/
END
```

```
      DOUBLE PRECISION FUNCTION XCOEF(U)
C        SUBROUTINE CALCULATES THE WELL FUNCTION FOR A LEAKY AGUIFER
C        GIVEN INPUT PARAMETERS OF U AND RB
C
C        THIS SUBROUTINE IS ACCURATE IN THE FOLLOWING RANGE:
C
C        FOR RB > 1.0         ACCURACY WITHIN 10%
C        FOR RB > 10.0        ACCURACY WITHIN 1%
      REAL*8 U,RB,XCOEF
      COMMON /MATH/ PI,EPS
      COMMON /PUSH/ RB
C
      XCOEF=DSQRT(PI/(2*RB))*DEXP(-RB)
     $ *DERFC(-(RB-2*U)/(2*DSQRT(U)))
      RETURN
      END
```

REFERENCES

Bachmat, Y., and Bear, J., The General Equations of Hydrodynamic Dispersion in Homogeneous Isotropic Porous Mediums, J. Geophys. Res., 69, 2561-2567, 1964.

Bear, J., Hydraulics of Groundwater, McGraw-Hill Inc.,New York, 1979.

Bear, J., and G. Dagan, Moving Interface in Coastal Aquifers, J. Hydraul. Div., Amer. Soc. Civil Eng., 90 (HY4), 193-216, 1964.

Benedict, B.A., H. Rubin, and S.A. Means, Movement of Salt and Hazardous Contaminants in Groundwater Systems, Water Resources Res., 71, 1983.

Benedict, B. A., J. L. Anderson, and E. L. Yandell, Analytical Modeling of Thermal Discharges: A Review of the State of the Art, Argonne National Laboratory, Report No. ANL/ES-18, April, 1974, 321 p.

CH_2M Hill Publication, Injection Wells in the State of Florida, Engineered by CH_2M Hill, 1983.

Calderon, M.R., Saltwater Intrusion Potential in Southwest Florida, M.E. Thesis, Dept. of Civil Engineering, University of Florida, Gainesville, Fla., 1982.

Christensen, B.A., Mathematical Methods in Analysis of Fresh Water Lenses in the Coastal Zones of the Florida Aquifer, Water Resources Res., 44, 1978.

Dagan, G., Pertubation Solutions of the Dispersion Equation in Porous Medium, Water Resources Res., 7 (1), 135-142, 1971.

Dagan, G. and J. Bear, Solving the Problem of Interface Upconing in a Coastal Aquifer by the Method of Small Pertubation, J. Hydraul. Res., 6(1), 15-44, 1968.

Eldor, M. and G. Dagan, Solutions of Hydrodynamic Dispersion in Porous Media, Water Resources Res., 8(5), 1316-1331, 1972.

Gelhar, L.W., and M.A. Collins, General Analysis of Longitudinal Dispersion in Nonuniform Flow, Water Resources Res., 7 (6), 1511-1521, 1971.

Ghyben, B.W., and J. Drabbe, Nota in verband met de voorgenomen putboring nabij Amsterdam, Tijdscrift von het koninklujk Institut von Ingeniurs, The Hague, Netherlands, 8-22, 1888.

Hantush, M.S., Unsteady Movement of Freshwater in Thick Unconfined Saline Aquifers, Bulletin of the I.A.S.H., 13 (2), 40-48, 1968.

Hantush, M.S. and C.E. Jacob, Non-steady Radial Flow in an Infinite Leaky Aquifer, Trans. Am. Geophys. Union, 36 (1), 95-100, 1955.

Helpling, C. L., Deep Well Injection In Florida, Proceedings of a Southeast Regional Conference on Ground Water Management, January 30-31, 1980, 152-163.

Herzberg, B., Die Wasserversorgung einiger Nordscebader, Jour. Gasbeleuchtung und Wasserversorgung, 44, 815-819, 842-844, 1901.

Hickey, J.J., Hydrology and Results of Injection Tests at Waste Injection Test Sites in Pinellas County, Florida, U.S. Geological Survey, Water Supply Paper 2183, 1982.

Hubbert, M. K., The Theory of Ground-Water Motion, The Journal of Geology, Volume 48, No. 8, 785-944, 1940.

Hunt, B., Dispersive Sources in Uniform Groundwater Flow, Journal of the Hydraulics Division, ASCE, Vol. 104, No. 1, Proc. Paper 13467, 75-85, January, 1978.

Hunt, B., Dispersion Calculation in Nonuniform Seepage, J. of Hydrology, 36, 261-277, 1978.

INTERCOMP Resource Development and Engineering, Inc., A Model for Calculating Effects of Liquid Waste Fisposal in Deep Saline Aquifer, U.S. Geological Survey Water Resources Investigation 76-61, 1976.

Koh, R.C.Y., Stratified Flow Towards a Sink in a Porous Medium, W.M. Keck Lab. of Hydro. Water Res., Tech. Mem. 64-2, California Inst. of Tech, 1964.

Kohout, F. A., Cyclic Flow of Salt Water in the Biscayne Aquifer of Southeastern Florida, J. Geophys. Res., 65(7), 2133-2141, 1960.

List, E.J., The Stability and Mixing of a Density Stratified Horizontal Flow in a Saturated Porous Medium, W.M. Keck Lab. of Hydr. Water Res., Report No. KH-R-11, California Inst. of Tech., 1965.

List, E.J., A Two-dimensional Sink in a Density Stratified Porous Medium, J. Fluid Mech., 33 (3), 529-543, 1968.

Lohman, S.W., and others, Definitions of Selected Ground-Water Terms -- Revisions and Conceptual Refinements: U.S. Geological Survey Water Supply paper, 1988, 21 p., 1972.

Means, S.A., Numerical Simulation of Aquifer Mineralization in Northeastern Florida, M.E. Thesis, Dept. of Civil Engineering, University of Florida, Gainesville, Florida, 1982.

Merritt, M.L., Subsurface Storage of Freshwater in South Florida: A Digital Model Analysis of Recoverability, U.S.G.S. Openfile Report #83-536, 1983.

Morton, B. R., On a Momentum-Mass Flux Diagram for Turbulent Jets, Plumes, and Wakes, Journal of Fluid Mechanics, 10, 1, 101-112.

Muskat, N., and R.D. Wychoff, An Approximate Theory of Water-Coning in Oil Production, Trans. Am. Inst. Mining Met. Engrs., 114, 1937, 144-163.

Peaceman, D.W., and H.H. Rachford, The Numerical Solution of Parabolic and Elliptic Differential Equations, J. Soc. Indust. App. Math.,3, 28-41, 1955.

Pinder, G.F., and Cooper, H.H., A Numerical Technique for Calculating the Transient Position of the Saltwater Front, Water Resour. Res., 6 (3), 875-882, 1970.

Puri, H.S. and Vernon, R.O., Summary of the Geology of Florida and a Guideline to the Classic Exposures: Florida Geological Survey Special Publication 5, 312 p. 1964.

Rubin, H., On the Application of the Boundary Layer Approximation for the Simulation of Density Stratified Flows in Aquifers, to be Published in Advances in Water Resources, 1982.

Rubin, H., and G.F. Pinder, Approximate Analysis of Upconing, Advances in Water Resources, 1, 97-101, 1977.

Segol, G., G.F. Pinder, and W.G. Gray, A Galerkin Finite Element Technique for Calculating the Transient Position of the Saltwater Front, Water Resources Res., 11 (2), 343-347, 1975.

Strack, O. D. L., A Single-Potential Solution for Regional Interface Problems in Coastal Aquifers, Wat. Resour. Res., 12(6), 1165-1174, 1976.

Theis, C.V., The Relationship Netween the Lowering of the Piezometric Surface and the Rate and Duration of Discharge of a Well Using Groundwater Storage, Trans. Amer. Geophys. Union, 2, 519-524, 1935.

Wheatcraft, S.W., and F.L. Peterson, Numerical Modeling of Liquid Waste Injectim into a Two-Phase Fluid System: University of Hawaii at Manoa, Water Resources Research Center, Technical Report No. 125.

Wilson, J.L., and P.J. Miller, Two-Dimensional Plume in Uniform Groundwater Flow, Journal of the Hydraulics Division, American Society of Civil Engineers, 108, No. HY4, 503-514, April, 1982.

Wooding, R.A., Convection in a Saturated Porous Medium at Large Rayleigh Number or PéClet Number, J. Fluid Mech., 15, 527-544, 1963.

Wooding, R.A., Mixing Layer Flows in a Saturated Porous Medium, _J. Fluid Mech., 19_, 103-112, 1964.